Pseudotyped vesicular stomatitis virus for analysis of entry of arenaviruses and its application to serodiagnosis of Argentine hemorrhagic fever

(水疱性口内炎ウイルスのシュードタイプを用いたアレナウイルスの
細胞侵入過程の解析とアルゼンチン出血熱の血清診断法への応用)

Koichiro Iha

伊波　興一朗

Contents

General Introduction

Viral hemorrhagic fever (VHF) is a serious illness characterized by extensive vascular damage and bleeding diathesis, fever, and multiple organ dysfunction. Infection of variety of viruses results in similar clinical manifestation of VHF, however, mode of transmission, reservoir animals and clinical outcome including fatality rate in humans are different among VHFs (Paessler *et al*., 2012).

These viruses causing VHF are distributed throughout four virus families, the *Arenaviridae*, *Bunyaviridae*, *Filoviridae*, and *Flaviviridae*. Several of these viruses cause severe VHF with high morbidity and mortality and can be highly infectious by aerosol dissemination, promoting serious concern about weaponization of these pathogens (Paessler *et al*., 2012).

In Japanese, under a Law concerning the Prevention of Infections and Medical Care for Patients of Infections which was enacted and become effective in 1999 associated with repeal of the old communicable disease control law, Ebola hemorrhagic fever, Marburg hemorrhagic fever, Crimean Congo hemorrhagic fever, South American hemorrhagic fever, Lassa fever, Smallpox and Plague are classified as Class 1 infectious diseases, which make the highest risk when outbreaks occurred in Japan. Among causative agents of these VHFs, Ebola virus, Marburg virus, Crimean Congo hemorrhagic fever virus, Lassa virus, South American hemorrhagic fever virus and

Variola virus are classified in Category 1 pathogens and are restricted to be handled in biosafety level 4 (BSL-4) containment laboratories in many countries including Japan.

Amongst Category 1 pathogens, Lassa virus and South American hemorrhagic fever virus, which consists of 5 virus species, are arenaviruses. Arenavirus belongs to a family *Arenaviridae* that is characterized by an envelope structure and a sandy (Latin, *arenosus*) appearance of the ribosomes seen in the sections of virions under electron microscopic observation. Arenavirus has a bisegmented ambisense single-stranded RNA genome and replicates in the cytoplasm of infected cells. Genome RNA of arenavirus consists of small (S) segment and large (L) segment. S segment RNA encodes a viral glycoprotein (GP) precursor (GPC) in a positive sense with respect to mRNA and a nucleocapsid protein (NP) in a negative sense, while L segment RNA encodes an L polymerase in a negative sense and a small RING finger protein (Z) in a positive sense. The NP coding region and the L coding region are transcribed into a genomic complementary mRNA. In contrast, the GPC coding region and Z coding region are transcribed into genomic-sense mRNA from corresponding antigenomic RNA, which also function as replicative intermediates (Emonet *et al*., 2009) and this ambiguous coding strategy is called "ambisense".

The family *Arenaviridae* is classified into two complexes, New World (NW) and

Old world (OW) arenaviruses, based on serologic, genetic, and geographic relationships and their hosts (Bowen *et al.*, 1997, Moncayo *et al.*, 2001). The natural reservoirs of hemorrhagic fever causing arenaviruses are known to be rodents. The NW arenaviruses are associated with rodents in the subfamily *Sigmodontinae* of the family *Cricetidae*, and NW complex is further divided into 3 major clades (A, B and C). Clade B contains 5 hemorrhagic fever causing arenaviruses, Junin virus (JUNV), Guanarito virus (GTOV), Sabia virus (SABV), Machupo virus (MACV) and Chapare virus (CHPV), which are known to cause South American hemorrhagic fever in humans (Delgado *et al.*, 2008). Of the OW arenaviruses, Lassa virus (LASV) and lymphocytic choriomeningitis virus (LCMV) are known to cause severe disease in humans (Buckley *et al.*, 1970, Barton *et al.*, 2000). Recently, another OW arenavirus, Lujo virus, was isolated in association with VHF emerged in Africa (Briese *et al.,* (2009) Genetic detection and characterization of Lujo virus, a new hemorrhagic fever-associated arenavirus from southern Africa (Briese *et al.,* 2009, Paweska *et al.*, 2009). It is estimated that 100,000 to 500,000 cases of Lassa virus infection occur each year in Western Africa, causing approximately 5,000 deaths (Idemyor *et al.*, 2010). The natural reservoirs of LASV and LCMV are rodents of the genus *Mastomys* and *Mus musculus*, respectively, however, natural reservoir of Lujo virus is unknown. Hemorrhagic fever arenaviruses are thought

to infect human through direct contact with the natural reservoirs, their excretions including urine or their blood, and viruses can be transmitted to other humans through mucosal contact, cutaneous contact or nosocomial contamination (McCormick *et al*., 1987).

Currently, there are no specific treatments approved for use against arenavirus hemorrhagic fevers. Present disease management consists of general supportive care; monitoring and correcting fluid, electrolyte and osmotic imbalances and treating hemorrhage with clotting factor or platelet replacement (Ogbu *et al*., 2007, Charrel *et al*, 2003). Convalescent immune serum therapy may be effective in treating cases of VHFs caused by Junin and Machupo virus infection, but the availability of such serum is extremely limited (Maiztefui *et al*., 1979, Harrison *et al*., 1999).

The only arenaviral hemorrhagic fever for which studies have been undertaken toward development of a vaccine has been Argentine hemorrhagic fever (AHF) caused by Junin virus. A live-attenuated vaccine, called Candid #1, has been evaluated in controlled trials among agricultural workers in AHF-endemic areas, where it appeared to reduce the number of reported AHF cases with no serious side effects (Ambrosio *et al*., 2011). It is not known if the Candid #1 vaccine would be effective against other South American hemorrhagic fevers and this vaccine is available only in Argentine.

As these viruses are categorized into BSL4 pathogens in many countries thus can be handled only in specific institutions with BSL4 facilities, analysis of pathogenesis of these pathogenic arenaviruses, development of therapeutic agents and vaccines for arenaviral hemorrhagic fevers have been impeded. In addition, epidemic areas of these diseases are mainly located in developing countries, that is, Sub-Saharan Africa and South America. Pharmaceutical companies have not been given their prior attention to develop medicines for these infectious diseases because of the profits generated from them.

To solve these problems, in Chapter 1 of the study, I developed vesicular stomatitis virus (VSV) pseudotypes bearing the respective envelope proteins of JUNV and LASV and examined their characterization especially focused on their attachment and entry to the susceptible cells. The VSV pseudotype mimics the infection process of JUNV or LASV, however, a gene encoding the envelope protein of JUNV or LASV is not encoded in VSV gene. Thus the VSV pseudotypes do not produce infectious progeny virus, so that they can be safely handled in a BSL2 containment level. The results found in chapter 1 indicated that the VSV pseudotypes were useful for studying function of arenavirus envelope proteins with respect to the biological functions including receptor binding and entry of ribonucleoproteins in cytoplams.

In Chapter 2, I established recombinant antigen-based serological diagnosis systems for AHF and I further analyzed the cross-reactivity of antibodies in the AHF patients' sera with other arenaviruses. The results found in this chapter indicated that the recombinant antigen-based serological diagnosis systems were useful in serodiagnosis of AHF suspected patients. Neutralization test (NT) using VSV pseudotype is found to be useful not only for serological diagnosis of AFH but also for differential diagnosis among South American hemorrhagic fever.

Chapter 1

Characterization of Pseudotype Vesicular Stomatitis Virus (VSV) bearing New and Old World Arenavirus Glycoprotein

ABSTRACT

Arenaviruses are a major cause of VHFs endemic to Sub-Saharan Africa and South America, and thus one of major public health and medical concerns in these regions. Because these arenaviruses causing VHFs, LASV, JUNV, GTOV, SABV, MACV and CHPV, are categorized in a biosafety level 4 (BSL4) pathogens, which is restricted to be cultured in a BSL facilities, biological studies including analysis of pathogenesis of these pathogenic arenaviruses, therapeutic drug or vaccine development have been impeded. Due to the difficulties to handle with these infectious viruses, VSV pseudotypes transiently bearing arenavirus envelope proteins has been developed as a surrogate virus system. In this chapter, I have developed VSV pseudotypes bearing LASV envelope protein (LASpv) and JUNV envelope protein (JUNpv), respectively. LASpv and JUNpv generated in several mammalian cell lines exhibited high infectivity in various mammalian cell lines. Arenaviral envelope proteins on the VSV pseudotypes were glycosylated by high-mannose type oligosaccharide. Endosomal low pH-induced endocytosis of pseudotype VSVs was confirmed by the use of lysosomotropic agents. Low pH induced membrane fusion by Lassa and Junin envelope protein was monitored by syncytium formation and reporter gene activities. The infection of JUNpv to Huh7 cells was mediated by binding to human transferrin receptor 1 (hTfR1) as a receptor.

Involvement of cathepsin L in JUNpv cell entry was suggested. These results indicate that the pseudotype VSVs developed in this study can be used to study arenavirus envelope proteins with respect to the biological functions including receptor interaction in the entry process.

INTRODUCTION

As described in "General Introduction", the family *Arenaviridae* consists of two complexes, NW arenaviruses and OW arenaviruses. LASV of OW arenavirus and JUNV, GTOV, SABV, MACV of NW arenavirus are known to cause VHF, Lassa fever, AHF, Venezuelan hemorrhagic fever (HF), Brazilian HF and Bolivian HF, respectively. AHF, Venezuelan HF, Brazilian HF and Bolivian HF are generically called South American HF (Paessler *et al*., 2012). Newly identified CHPV is also causative agent of South American HF in Bolivia (Delgado *et al*., 2008). More recently, another OW arenavirus, Lujo virus, was isolated from VHF patients in Africa and the virus was shown to be genetically distinct from other OW arenaviruses (Briese *et al*., 2009).

Since these highly pathogenic viruses require manipulation under high-level containment (BSL4), researches on these viruses are highly restricted, and for these reasons, detailed knowledge of arenavirus life-cycle has still been limited. Therefore, some alternative research tools for these viruses are needed to develop new therapies and preventives for arenavirus hemorrhagic fevers.

To solve these problems, VSV pseudotype bearing arenavirus GP is thought to be an excellent candidate for use in studying these pathogenic arenaviruses. A recombinant

VSV lacking its own envelope (G) gene has been used to produce a pseudotype or recombinant VSV possessing the envelope proteins of heterologous viruses. These viruses possess a reporter gene instead of a VSV G gene in its genome, and therefore it is easy to evaluate their infectivity in the study of viral entry, including identification of viral receptors (Tani *et al*., 2010, Whitt MA, 2010). Furthermore, advantage can be taken of a property of the VSV pseudotype, which is competence for single-round infection, in handling many different viruses that are either difficult to amplify in cultured cells or animals or that require specialized containment facilities.

In this chapter, I generated a novel VSV pseudotype bearing JUNV glycoproteins (JUNpv), and confirmed whether JUNpv can be used to analyze the function of arenavirus glycoprotein with respect to the biological functions including receptor interaction in the entry process. In addition, by using the JUNpv, I investigated the entry mechanisms of the pathogenic arenaviruses.

MATERIALS AND METHODS

Construction of Plasmids

The glycoprotein precursor (GPC) cDNAs of JUNV (MC2 strain) and LASV (Josiah strain) were kindly supplied from Prof. V Romanowski, Universidad Nacional de La Plata and Prof CJ Peters, UTMB, respectively, The GenBank accession numbers of the nucleotide sequences of JUN GP and LAS GP genes are U70799 and J04324, respectively. The GP cDNAs of the JUNV and LASV were cloned into the expression vector, pKS336 (Saijo *et al*., 2002). The resulting plasmids were designated pKS-JUNV-GP and pKS-LASV-GP, respectively. Each GP sequence of the plasmids was confirmed to be identical to the original cDNA sequence using ABI PRISM® 3100-Avant Genetic Analyzer (Applied biosystems).

FLAG/One-STrEP (FOS) tagged fusion protein expression vectors were also constructed. Stop codon deleted cDNAs of the JUNV-GP and LASV-GP were synthesized by PCR from each cDNAs described above. The PCR products were cloned into pCAG-MCS2-FOS, which expresses carboxyl-terminal FOS-tagged fusion protein (provided by E. Morita, Osaka University). The resulting plasmids were designated pCAG-JUNV-GP-FOS and pCAG-LASV-GP-FOS, respectively. The cDNA encoding G

protein (G) of VSV was amplified by PCR from pCAG-VSV-G and cloned into pCAG-MCS2-FOS to pCAG-VSV-G-FOS.

A plasmid expressing hTfR1 was also generated. Total RNAs were isolated from 293T cells with TRIzol Reagent (Invitrogen, Carlsbad, CA) according to the manufacturer's instructions. The cDNA was synthesized by reverse transcription with Superscript III reverse transcriptase (Invitrogen) using random hexamer primers (Invitrogen). The cDNA encoding hTfR1 was amplified by PCR with Expand High Fidelity PCR System (Roche Applied Science, Indianapolis, IN) using the cDNA synthesized from 293T RNAs. Amplified cDNA was cloned into pKS336. The resulting plasmid was designated as pKS-hTfR1. The cloned sequence was confirmed to be identical to hTfR1 cDNA sequence using ABI PRISM® 3100-Avant Genetic Analyzer.

Cells

The hamster (BHK and CHO), mouse (NIH3T3 and NMuLi), monkey (VeroE6), human (Huh7, 293T, HeLa, Molt-4 and Jurkat) cell lines were obtained from the American Type Culture Collection (Rockville, MD) or DS Pharma Biomedical Co. Ltd. (Osaka, Japan). All cell lines except for lymphocytes, Molt-4 and Jurkat, were grown in Dulbecco's modified Eagle's medium (DMEM; Sigma-Aldrich, St. Louis, MO)

containing 5% heat inactivated fetal bovine serum (FBS). All lymphocytes were grown

in RPMI 1640 (Sigma-Aldrich) containing 10% FBS. To establish a CHO cell line

stably expressing human TfR1 (CHO/TfR1), CHO cells were transfected with

pKS-hTfR1 by Fugene HD (Roche) reagent. The transfected CHO cells were selected

with DMEM containing 5% FBS and 2 µg/ml of Blasticidin S-HCl (Invitrogen). When

clusters of the cells were appeared, some clusters of the cells were cloned and

subcultured to establish CHO/TfR1.

Generation of VSV pseudotypes

VSV Pseudotypes bearing GP of Junin virus and Lassa virus, VSVG (VSVpv),

and murine leukemia virus envelope proteins (MLVpv) were generated as described

previously (Tani *et al*., 2007). Briefly, 293T cells were grown to 70% confluence on

collagen-coated tissue culture plates, then transfected with pCAG-JUNV-GP-FOS,

pCAG-LASV-GP-FOS, pCAG-VSV-G-FOS, and pFBASALF, which expresses murine

leukemia virus envelope proteins (provided by T. Miyazawa, Kyoto University),

respectively. After 24 hr of incubation, the transfected cells were infected with

G-complemented (*G) VSVΔG/Luc (*G-VSVΔG/Luc) (Tani *et al*, 2010) at a

multiplicity of infection (MOI) of 0.1. One hr after incubation, virus-containing medium

was aspirated and the cells were extensively washed four times with serum-free DMEM to remove seed virus. After 24 hr of incubation, the culture supernatants containing VSV pseudotypes were centrifuged to remove cell debris and stored at -80°C until use.

The infectivities of JUNpv, LASpv, VSVpv and MLVpv were assessed by luciferase activity. For luciferase assay, the relative light unit (RLU) value was determined by using the Bright-Glo luciferase assay system (Promega Corporation, Madison, WI), following a protocol provided by the manufacturer.

Western blotting

293T cells were transfected with each of pCAG-JUNV-GP-FOS, pCAG-LASV-GP-FOS, and pCAG-VSV-G-FOS. Twenty four hours (hr) after transfection, the cells were collected by pipetting and washed with phosphate buffered saline (PBS) three times. Then, the cells were lysed in PBS containing 1% NP40 for 1 hr at room temperature. Cell lysates were centrifuged at 3,000 rpm for 10 minutes (min) to separate insoluble pellets from supernatants. The supernatants were used as samples. VSV pseudotypes generated as described above were pelleted through a 20% (wt/vol) sucrose cushion at 25,000 rpm for 2 h by using an SW28 rotor (Beckman Coulter, Tokyo, Japan). The pellets were resuspended in phosphate-buffered saline (PBS) and

also used as samples.

Each sample was mixed with equal volume of Tris-Glycine SDS Sample Buffer (2x) (Invitrogen), boiled for 5 min, then the proteins in the samples were separated by 10% SDS-polyacrylamide gel electrophoresis at 100 V for 90 min and the proteins were transferred to a methanol activated polyvinylidene difluoride (PVDF) membrane (Millipore, Billerica, MA) using a semi-dry blotter (Atto, Tokyo, Japan) at 200 mA for 30 min. The membranes were then blocked in PBS containing 0.5% Tween20 (Sigma Ardrich) and 5% skim milk (Yukijirushi, Japan) (SKIM-PBS-T) at room temperature for 1 hr. Then the membrane was incubated with mouse monoclonal anti-FLAG antibody (Sigma) at a dilution of 1 in 1,000 at room temperature for 1 hr, followed by washing with PBS-T and incubated at room temperature for 1 hr with HRP-conjugated goat anti-mouse immunoglobulin (Zymed, Invitrogen) at a dilution of 1 in 5,000 with SKIM-PBS-T and washed three times in PBS-T. The reactions were visualized with a SuperSignal West Dura Extended Duration Substrate (Pierce, Rockford, IL) using an LAS3000 analyzer (Fuji Film, Tokyo, Japan).

Immunofluorescence assay (IFA)

CHO/hTfR1 cells were dispersed by trypsinization, washed three times in PBS,

spotted on 14-well HT-Coated slide glasses (AR Brown Co., Ltd., Tokyo, Japan), air

dried, and fixed with acetone at room temperature for 5 min. The slides were stored at

-80 °C until use. Slide glasses with the parental CHO cells were also prepared as

negative control. For the IFA, mouse anti-hThR1 antibody (BD Biosciences, San Jose,

CA) at a dilution of 1 in 1,000 were placed on the wells of both CHO/hTfR1 slides and

parental CHO slides, and the slides were incubated under humidified conditions at 37°C

for 1 hr. After washing in PBS, the antigens were reacted with fluorescein

isothiocyanate (FITC)-conjugated goat anti-mouse IgG antibody (1:200; Zymed). After

washing in PBS, the slides were examined for the staining pattern under a fluorescent

microscope (Zeiss, Oberkochen, Germany) with appropriate barrier and excitation

filters for FITC visualization.

Analysis of glycosylation of the envelope proteins

To examine the effects of oligosaccharide modification of JUNV-GP and

LASV-GP, the cell lysates and the purified pseudotype virions were digested with

endoglycosidase H (Endo H) or peptide-N-glycosidase F (PNGase F) (Roche),

following a protocol provided by the manufacturer, and analyzed by western blotting.

Effects of various inhibitors of endosomal acidification on JUNpv infection

Huh7 cells were treated with various concentrations of inhibitors of endosomal acidification; bafilomycin A$_1$ (SIGMA), ammonium chloride (SIGMA), or chloroquine (SIGMA) for 1 hr at 37˚C, then the cells were infected with JUNpv, LASpv, VSVpv and MLVpv, respectively, at an MOI of 1 and further cultured for 24 hr. Lusiferase activity in the cells were measured as described above.

Cell fusion assay

Huh7 cells were transfected with pCAG-JUNV-GP-FOS, pCAG-LASV-GP-FOS or pCAG-VSV-G. Twenty-four hr after transfection, the cells were rinsed once with PBS and then incubated with citrate-phosphate buffers adjusted to the indicated pH values for 2 min. The citrate-phosphate buffers were then replaced to DMEM containing 5% FBS, and incubated for 24 hr for JUNV-GP or LASV-GP expressing cells or 8 hr for VSV-G expressing cells. Then the cell monolayers were observed for the induction of cell fusion using BZ-9000 microscope (Keyence, Osaka, Japan). Huh7 cells of the same condition were also transfected with a plasmid encoding GFP as indicators of transfection efficiency, then these cells were analyzed for the expression of GFP using BZ-9000 microscope.

Quantitative cell fusion assay

The 293T cells were grown on 35-mm tissue culture plates and transfected with pCAG-JUNV-GP-FOS, pCAG-LASV-GP-FOS and pCAG-VSVG, respectively, together with pCAGT7pol (provided by Prof. Y. Matsuura, Osaka University), an expression plasmid encoding T7 RNA polymerase gene under control of the CAG promoter (Takikawa *et al.*, 2000). The target cells, Huh7, were separately grown on 35-mm tissue culture plates and transfected with pT7EMCVLuc (provided by Y. Matsuura), a reporter plasmid encoding a firefly luciferase gene under control of the T7 promoter. After 24 hr of transfection, the target cells were collected by trypsinization, and re-grown in a 96-well plate. The 293T cells were collected by pipetting with 0.05% EDTA in PBS, and suspended in DMEM containing 5% FBS. The 293T cells were overlaid onto the target Huh7 cells and incubated for 4 hr. The co-cultured cells were bathed in citrate-phosphate buffers at pH 3.0, 4.0, 5.0, 6.0 or 7.0 for 2 min, then were added with DMEM containing 5% FBS and incubated for 12 hr. The cell fusion activity was quantitatively determined by measuring luciferase gene expression in the lysates of the co-cultured cells. The RLU value was determined by using the Bright-Glo luciferase assay system as described above.

Inhibition of JUNpv infection by anti-TfR1 antibody or ferric ammonium citrate

Huh7 cells were pretreated with various concentration of anti-hTfR1 for 1 hr at 37˚C and infected with JUNpv, LASpv, VSVpv and MLVpv, respectively, at a MOI of 1. After 1hr of adsorption at 37˚C, the cells were washed, and cultured for 24 hr at 37˚C. Then, lusiferase activitiese in the cells were measured as described above.

Huh7 cells were pretreated with the various concentration of ferric ammonium citrate (FAC), which contains rich iron and known to decrease mRNA level of TfR (Ward *et al.*, 1982), and incubated at 37˚C. After 2 hr of incubation, the cells were infected with JUNpv, LASpv and VSVpv, respectively, as described above. Luciferase activities in the cells were measured as described above. after 24 hr of incubation at 37˚C.

Effects of various protease inhibitors on the infection of JUNpv

Cells were treated with various concentrations of protease inhibitors; Leupeptin (Calbiochem Merck, Darmstadt, Germany), Cathepsin inhibitor peptide (Calbiochem Merck), CA-074Me (Calbiochem Merck), Cathepsin L inhibitor peptide II (Calbiochem Merck) and Cathepsin L inhibitor peptide IV (Calbiochem Merck) for 1 hr at 37˚C, then infected with JUNpv, LASpv, VSVpv and MLVpv, respectively, at an MOI of 1 and

23

cultured for 24 hr. Then, lusiferase activities in the cells were measured as described

above.

RESULTS

Infectivities of JUNpv and LASpv generated in various cell lines

JUNpv, LASpv and VSVpv were generated from the expression plasmids of the envelope proteins of Junin virus, Lassa virus and VSV, respectively, by using established methods in various cell lines (Tani *et al*, 2010). To examine the infectivities of JUNpv, LASpv and VSVpv generated in various cell lines, JUNpv, LASpv and VSVpv were generated in 293T, Huh7, BHK and VeroE6 cells, respectively, and their infectivities were measured on either Huh7 or VeroE6 cells. First, I have analyzed the infectivities of JUNpv and LASpv generated in 293T cells on Huh7 and VeroE6 cells and found that their infectivities were comparable to those of VSVpv on both Huh7 and VeropE6 cells (Fig. 1-1). This result indicated that both Huh7 and VeroE6 cells were highly susceptible to the infection of JUNpv and LASpv, and also that JUNpv and LASpv were efficiently generated in the 293T cells. Then I have generated JUNpv and LASpv using Huh7, BHK, and VeroE6 cells. JUNpv and LASpv were efficiently generated in the Huh7 cells as in the 293T cells, however, they were generated less efficiently in the BHK and VeroE6 cells (Fig. 1-1).

25

Infection of JUNpv and LASVpv to various target cell lines

As Huh7 and VeroE6 cells were shown to be highly susceptible to the infection with JUNpv and LASpv, susceptibility of various cell lines to them were determined (Fig. 1-2). All of the cells analyzed were shown to be susceptible to JUNpv infection. Among them, CHO, VeroE6, Huh7, and HeLa cells exhibited the high susceptibility, while Molt-4, NIH3T3 and NMuLi cells did lower levels of susceptibility. Susceptibility of LASpv infection was similar in many cell lines but it is noteworthy that Jurkat cells were not susceptible to LASpv infection.

Glycosylation of Arenavirus GPs

To examine the glycosylation of LASV-GP and JUNV-GP expressed in Huh7 cells upon transfection of the plasmids generated in this study, the cell lysates and the pseudotype virions were treated with glycosidases; Endoglycosidase H (Endo-H) and PNGase F. Endo-H is a glycosidase that cleaves within the chitobiose core of high mannose from asparagine-linked (N-linked) glycoproteins. On the other hand, PNGase F is an amidase that cleaves between the innermost GlcNAc and asparagine residues of high mannose, hybrid, and complex oligosaccharides from N-linked glycoproteins. Sugar chains on both LASV-GP and JUNV-GP were sensitive to Endo-H and PNGase F,

since they were migrated faster on SDS-PAGE. The result indicated that they were glycosylated with N-linked high mannose type oligosaccharide. On the other hand,, sugar chain on VSV-G was sensitive to PNGase F but resistant to Endo-H, indicating VSV-G was glycosylated with complex type oligosaccharide (Fig. 1-3).

Involvement of endosomal acidification in infection of JUNpv and LASpv

To examine whether JUNpv and LASVpv represent entry mechanisms of original viruses, Huh7 cells were pretreated with various concentrations of inhibitors of endosomal acidification, bafilomycin A1, ammonium chloride and chloroquine, and then the cells were inoculated with LASpv, JUNpv and MLVpv, respectively, at an MOI of 1 (Fig 1-4). As expected, treatment with all of the reagents did not affect the infectivity of MLVpv, which enters the cells through a pH-independent direct fusion of the viral membrane and plasma membrane. In contrast, infections of JUNpv and LASpv as well as VSVpv, which enter cells through pH-dependent endocytosis, were inhibited by treatment with all of the reagents in a dose-dependent manner, suggesting that JUNpv and LASpv enter the cells through pH-dependent endocytosis.

pH dependent membrane fusion induced by JUNV-GP and LASV-GP

Huh7 cells were transfected with pCAG-LASV-GP-FOS, pCAG-JUNV-GP-FOS, and pCAG-VSV-G-FOS, respectively. After 24 hr post-transfection, the cells were treated with the citrate-phosphate buffer with various pH values for 2 min, then culture in DMEM containing 5% FBS. Syncytium formations were evident in the Huh7 cells expressing LASV-GP treated with pH4.0 while they were evident in the JUNV-GP expressing cells treated with pH5.0 or lower. They were evident in the cells expressing VSV-G treated with pH6.0 or lower (Fig. 1-5A).

To examine the pH dependent cell fusion activity of the Arenavirus envelope proteins, I utilized a highly sensitive and quantitative reporter gene activation method as established previously (Takikawa *et al*., 2000). Huh7 cells were transfected with pCAG-LASV-GP-FOS, pCAG-JUNV-GP-FOS and pCAG-VSV-G-FOS, respectively, together with pCAGT7pol. The transfected cells were treated at acidic pH condition for 2 min, then co-cultured with the reporter Huh7 cells that were transfected with pT7EMCVLuc, in which luciferase gene was expressed under the control of the T7 promoter. Thus, cell fusion of both cells can be quantitatively measured by the expression level of luciferase. As shown in Fig. 1-5B, LASV-GP induced cell fusion after treatment with pH4.0 or lower, and JUNV-GP did with pH5.0 or lower, while

VSV-G did with pH6.0 or lower.

Involvement of TfR1 in infection of JUNpv

The hTfR1 is demonstrated to be a principal entry receptor of clade B of NW arenaviruses including JUNV, MACV, SABV (Radoshitzky *et al*., 2007, Choe *et al*., 2011). To confirm whether the hTfR1 on the susceptible cells is utilized by infection of JUNpv, infection inhibition assays using anti-hTfR1 antibody were conducted. Huh7 cells were pretreated with various concentrations of anti-hTfR1 antibody for 1 h and then inoculated with LASpv, JUNpv and VSVpv, respectively. Infectivities were determined at 24 h post-infection by measuring the luciferase activity. The infections of both Huh7 cells with JUNpv were inhibited by anti-hTfR1 antibody in a dose dependent manner, whereas no inhibition of infections was observed for LASpv and VSVpv (Fig. 1-6A).

Infectivities of JUNpv on hTfR1 overexpressed cells were also examined. The CHO cells were transfected with pKS-hTfR1, then the cells expressing hTfR1 were selected and cloned with the medium containing Blasticidin S-HCl. The stable CHO-TfR1 cells (CHO/TfR1) were established and analyzed for the expression of hTfR1 by IFA and western blotting (Fig. 1-6B left panel). As can be seen, hTfR1 was

highly expressed on the cell surface of the CHO/TfR1 compared to the normal CHO cells. The CHO/TfR1 showed higher susceptibility to JUNpv infection compared to the normal CHO cells, while susceptibilities of the CHO/TfR1 cells and the normal CHO cells to infections of LASpv and VSVpv were substantially identical (Fig. 1-6B right panel).

Then, an effect of treatment of Huh7 cells with FAC, known to downregulate the expression of TfR1, on susceptibility of the cells to JUNpv infection was examined. As shown in Fig. 1-6C, the infection of JUNpv was reduced by FAC pretreatment in a dose dependent manner, while those of LASpv and VSVpv were not affected by FAC treatment.

These results indicated that as with JUNV, the VSV pseudotype harbouring JUNV-GP infected the susceptible cells using the hTfR1 as a principal receptor.

Involvement of cellular proteases in the infection of JUNpv

To examine the involvement of cellular protease in the infection of JUNpv, Huh7 cells were pretreated with various protease inhibitors, and inoculated with LASpv, JUNpv, VSVpv and MLVpv, respectively. Infections of all the VSV pseudotypes were not inhibited by pretreatment with leupeptin, which is the inhibitor of serine-threonine

protease and selectively inhibits trypsin, papain, cathepsines A and B, and some other

cellular proteases (Fig. 1-7A). On the other hand, only infection of JUNpv was inhibited

by cathepsin inhibitor peptide, Z-FG-NHO-Bz, which selectively inhibits cathepsines B

and L, and papaine in a dose dependent manner (Fig. 1-7B). To identify the protease

involved in JUNpv infection, the cells were pretreated with cathepsin B inhibitor

(CA-074Me), cathepsin L inhibitor II and cathepsin L inhibitor IV, respectively. As

shown in Fig. 1-7C, D, E, infection of JUNpv was inhibited by cathepsin L inhibitor II

and IV, but not by cathepsin B inhibitor. To confirm the involvement of cathepsin L in

JUNpv infection to other cell lines, an effect of pretreatment of VeroE6 and CHO/TfR1

cells with cathepsin L inhibitor II or cathepsin L inhibitor IV on JUVpv infection were

analyzed. As shown in Fig. 1-7F, infection of JUNpv was inhibited by cathepsin L

inhibitors in a dose dependent manner.

DISCUSSION

In this chapter, I developed VSV pseudotypes bearing LASV-GP and JUNV-GP, and examined their characterizations.

At first, I generated plasmids encoding the GP-FOS fusion proteins of LASV and JUNV. Although, in general, a tag fused viral protein often loses its function, LASpv and JUNpv bearing respective FOS-tagged-GP efficiently infected the variety of cells (Fig.1-1), indicating the FOS-tagged GPs properly functioned. JUNpv generated in several mammalian cell lines exhibited infectivity in various mammalian cell lines (Fig. 1-1). Especially, JUNpv generated in 293T cells and Huh7 cells exhibited highest infectivities (Fig. 1-1). As these arenavirus GPs with two tags (FLAG tag and One-STrEP tag), generated in this chapter, functioned in infection of the VSV psudotypes, it is likely that the tagged GPs were properly expressed and processed as with authentic arenavirus GPs. Thus, these proteins and the VSV pseudotypes are useful tools for investigating biological function of the GPs, virus-cell interaction and cell tropism of arenavirus.

It was demonstrated that LASpv and JUNpv infected almost all adherent cells derived from various tissues and animal species (Fig. 1-2). It may represent that all

adherent cells express receptor(s) for LASpv and JUNpv. However, infectivities to Jurkat cells were different between LASpv and JUNpv, that is, LASpv exhibited no infectivity to Jurkat cells. This result is in agreement with the previous study that showed Lassa virus infected almost all mammalian cells but not Jurkat cells (Garbutt *et al*., 2004, Rojek *et al*., 2007). These results indicate that pseudotype VSVs generated in this study represent the original tropism of Lassa virus and Junin virus.

Previous study demonstrated that both LASV-GP and JUNV-GP were glycosylated by N-linked high mannose type oligosaccharide (Albarino *et al*., 2009, Eichler *et al*., 2006), while VSV-G is glycosylated by complex type oligosaccharide (Spiro and Spiro. 2001, Marozin *et al*.,2012). In the present study, both LASV-GP and JUNV-GP expressed in the cells and on the VSV pseudotypes were sensitive to Endo-H and PNGase F treatment (Fig. 1-3), thus both JUNpv and LASpv were glycosylated by mannose type oligosaccharide. These data indicated that LASpv and JUNpv generated in this study possessed the same glycosylation type on their GPs as with original arenaviruses.

Using the VSV pseudotypes generated in the chapter, I examined whether the VSV pseudotypes mimicked the entry mechanisms of original arenaviruses. Previous study showed that infection of cells with LASV, LCMV and JUNV could be inhibited at

the entry stage by lysosomotropic weak bases (Glushakova et al., 1989, Borrow and

Oldstone, 1994, Castilla *et al*., 1994). Subsequent analysis of the pH-dependent fusion

of LCMV indicated that the GP spike is activated to a fusion active state by

conformational changes of the GP induced at low pH condition in the endosome then

induces fusion of virion membrane and endosomal membrane (Di Simone *et al*., 1994;

Di Simone and Buchmeier, 1995). In the present study, a pH-dependent infection of the

VSV pseudotypes was confirmed by the use of lysosomotropic agents (Fig. 1-4).

Low-pH induced membrane fusion by LASV-GP and JUNV-GP was investigated

in the previous study (Klewitz *et al*., 2007, Castilla and Mersich, 1996). Cell fusion of

LAS-GP-FOS and JUN-GP-FOS initiated with a low pH treatment was monitored as

syncytium formation and reporter gene activities (Fig. 1-5). These data indicated that

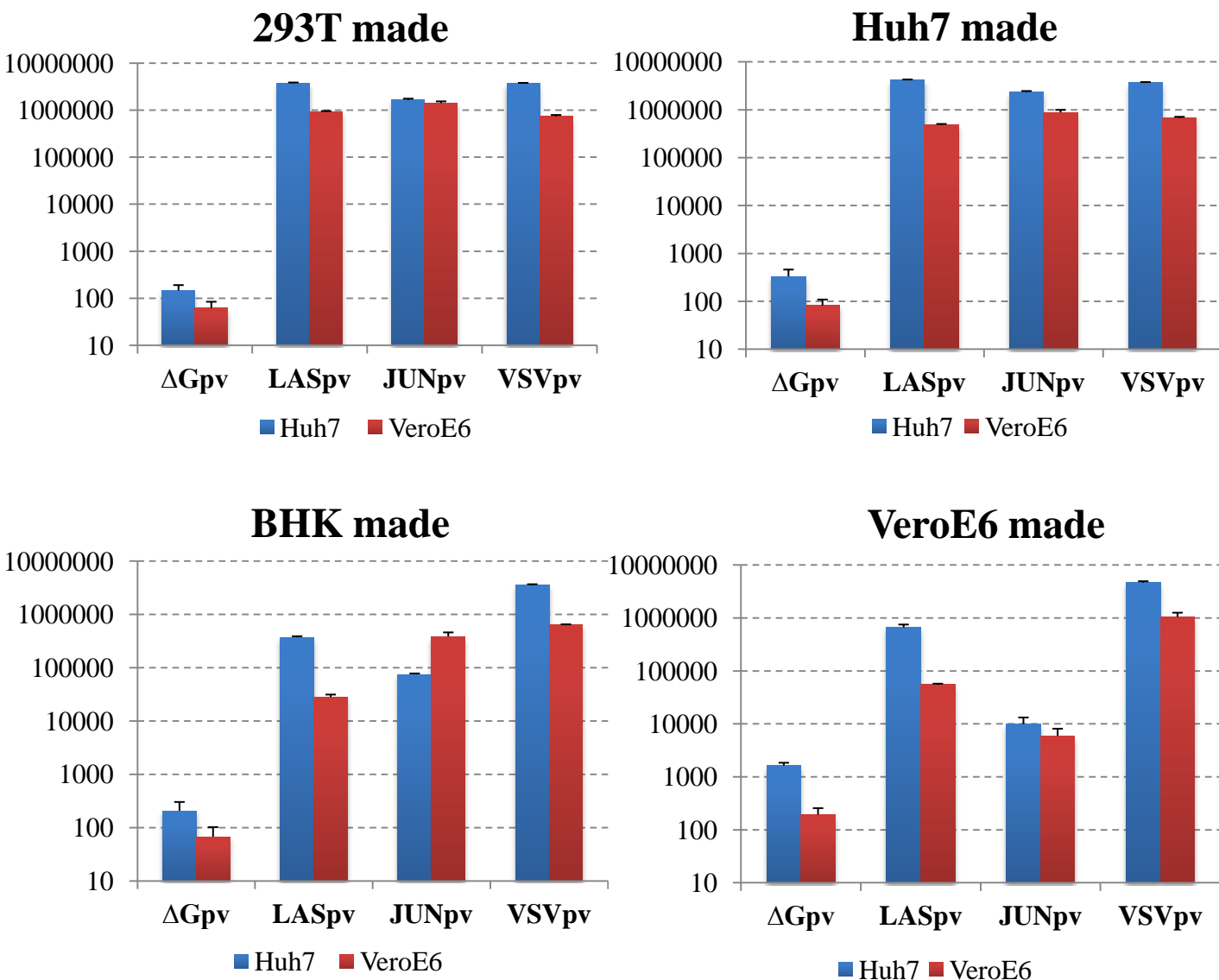LASpv and JUNpv entered the cells in the same manner as original arenaviruses.

Previous study shows that TfR1 is the principal cellular receptor for JUNV,

MACV, GTOV and SABV (Radoshitzky *et al*., 2007), and Chapare virus also utilizes

TfR1 for cell entry (Helguera *et al*., 2012). On the other hand, LASV and LCMV are

known to use α-dystroglycan (α-DG) as a principal cellular receptor (Cao *et al*., 1998).

However, there is a strong possibility that arenaviruses also use another unknown

receptor(s). Amapari virus and Tacaribe virus, non-pathogenic Clade B viruses, can

enter cells in α-DG- and TfR1- independent manner (Flanagan *et al*., 2008). It is also

known that some strains of LCMV do not use α-DG for their receptor (Smelt *et al*.,

2001). α-DG independent entry of LASV was also demonstrated (Shimojima *et al.,*

2012). In this study I confirmed that JUNpv useed TfR1 as an entry receptor but LASpv

did not. The observation is in agreement with the original arenaviruses. Thus, these

VSV pseudotypes are thought to be useful for investigating unknown entry receptor(s)

for Lassa virus and Junin virus.

It is known that cellular site-1 protease (S1P) activates the function of OW and

NW arenavirus GPCs by cleaving GPC into GP1 and GP2 (Rojek *et al*., 2008, Lenz *et*

al., 2001). The GPC cleavage is known to occur before virions are formed. However

some cellular proteases that potentiate arenavirus cell entry have not been examined

until now. In this study I demonstrated the involvement of cathepsin L in infection of

JUNpv (Fig. 1-7). This is the first report that demonstrated the use of cathepsin on

arenavirus infection. As cathepsin exists in lysosome / endosome, and I demonstrated in

Fig. 1-4 and Fig. 1-5 that endosomal acidification is crucial for cell fusion activity of

JUNV-GP, it is suggested that JUNV attaches the cells via TfR1 as the receptor, then is

internalized to the target cells by endocytosis, and finally cathepsin L in the endosome

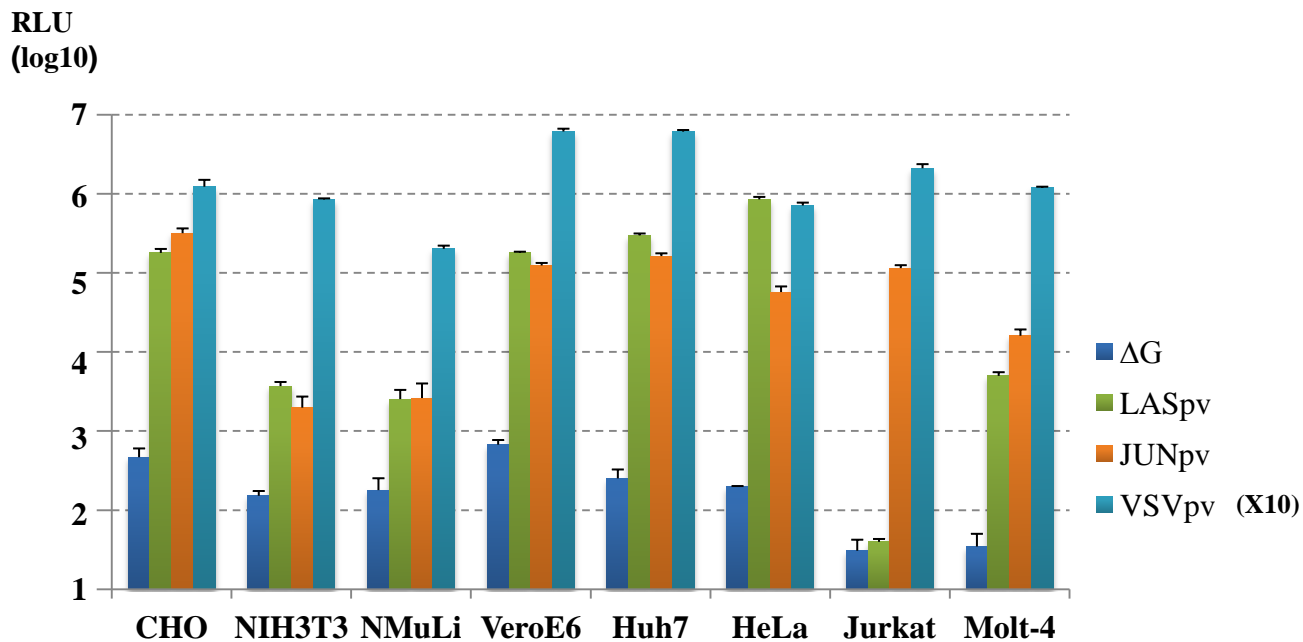activate the cell fusion activity of JUNV-GP to release the vairal ribonucleoprotein into

the cytoplasm.

In conclusion, characterizations of LASpv and JUNpv in this study revealed the VSV pseudotypes of arenaviruses mimicked the attachment, internalization and endosomal membrane fusion of infectious arenaviruses. Since many pathogenic arenaviruses causing VHF in human are classified in the BSL4 pathogens, the VSV pseudotypes of arenaviruses are quite useful to the further detailed examination on arenavirus entry mechanisms. Moreover, the VSV pseudotypes of arenaviruses may be applied for development of virus neutralization assay, a gold standard method to detect virus specific antibody responses in VHF patients, without using pathogenic arenaviruses. Such an application is to be shown in the next chapter.

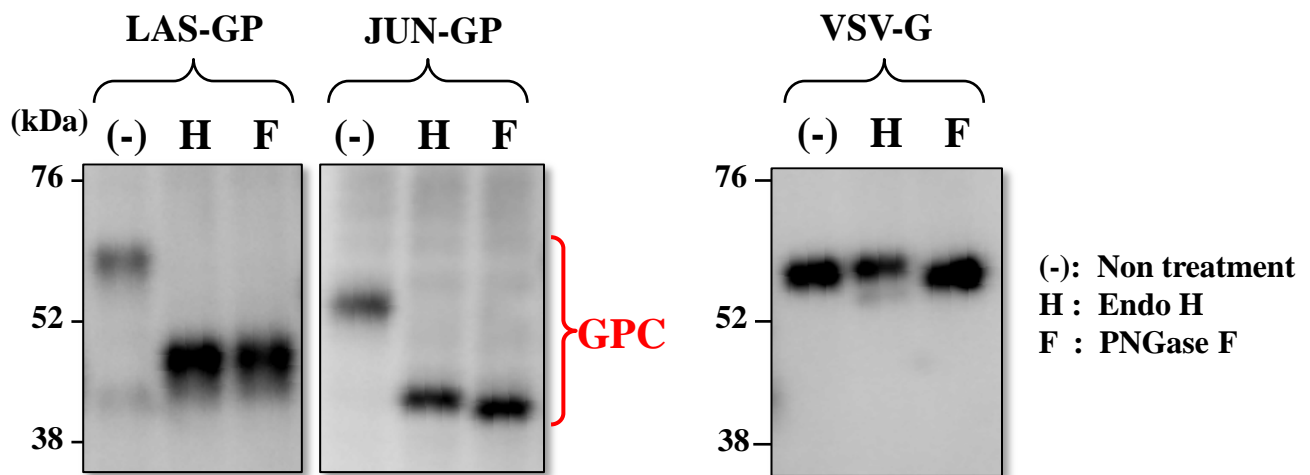**Figure 1-1. Infectivities of various VSV pseudotypes generated by various cell lines.**
Infectivities of LASpv and JUNpv generated in various cell lines (293T, Huh7, BHK and VeroE6 cels) were determined in Huh7 and VeroE6 cells by luciferase activity (RLU). VSV pseudotype without envelope protein (ΔG) was used as a negative control. The results shown are from three independent assays, with the error bars representing the standard deviations.
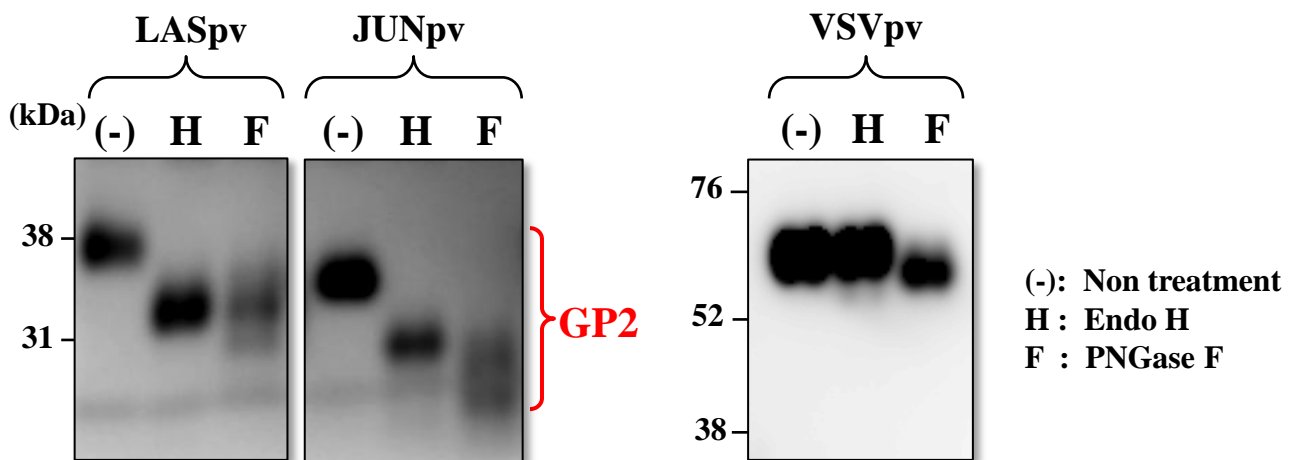
Figure 1-2. Susceptibility of various cells to VSV pseudotype infection.
LASpv and JUNpv generated in 293T cells were inoculated into indicated cell lines at an MOI of 1. After 24h post-infection, infectivities of the viruses were determined by relative luciferase units (RLU). The ΔG was used as a negative control. The results shown are from three independent assays, with the error bars representing the standard deviations.
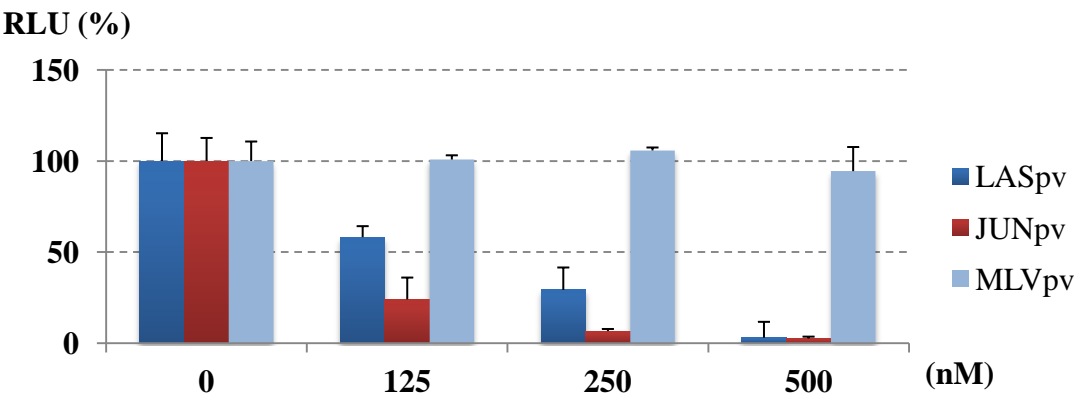
(A) Cell lysates

LAS-GP   **JUN-GP**   **VSV-G**

(kDa) (-) H F   (-) H F   (-) H F

GPC

(-): Non treatment
H : Endo H
F : PNGase F

(B) Purified virions

LASpv   **JUNpv**   **VSVpv**

(kDa) (-) H F   (-) H F   (-) H F

GP2

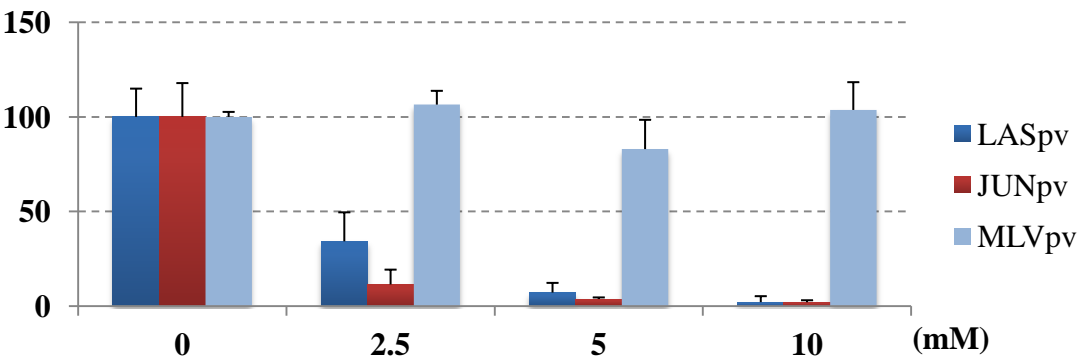(-): Non treatment
H : Endo H
F : PNGase F

Figure 1-3. Analysis for glycosylation of the envelope proteins
(A) Cell lysates derived from LAS-GP, JUN-GP or VSV-GP expressing cells and (B) purified LASpv,
JUNpv or VSVpv were digested with endoglycosidase H (Endo H) or peptide-N-glycosidase F
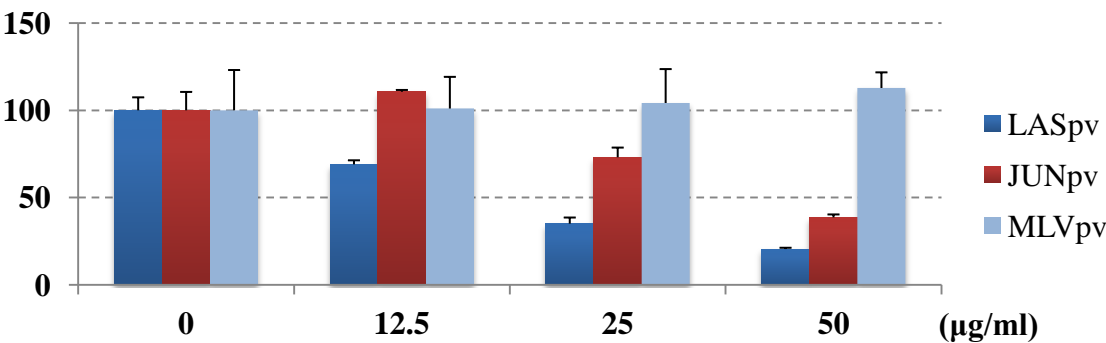(PNGase F), and analyzed by Westernblotting.
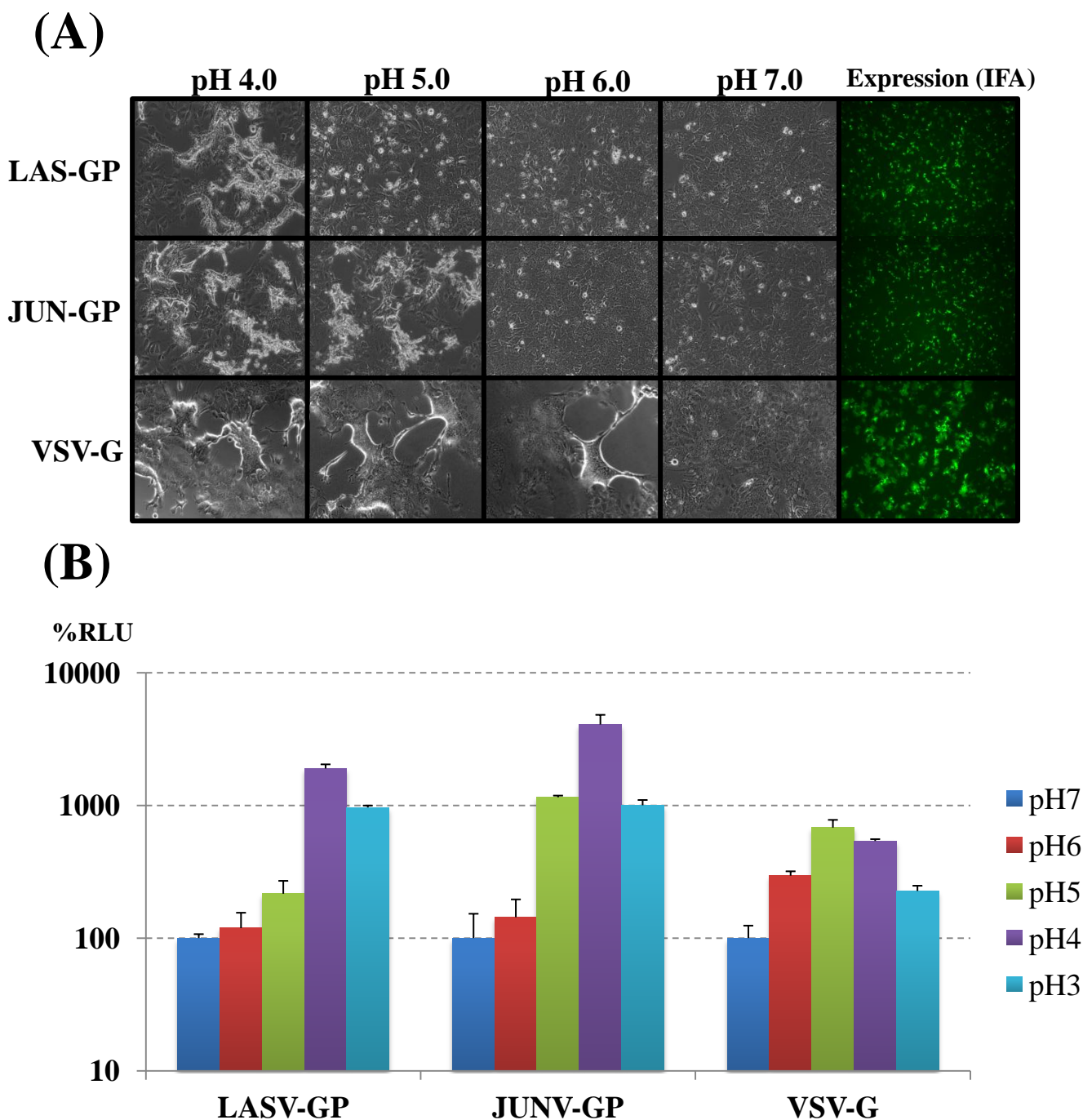
(A) Bafilomycin A1

(B) Ammonium chloride

(C) Chloroquine

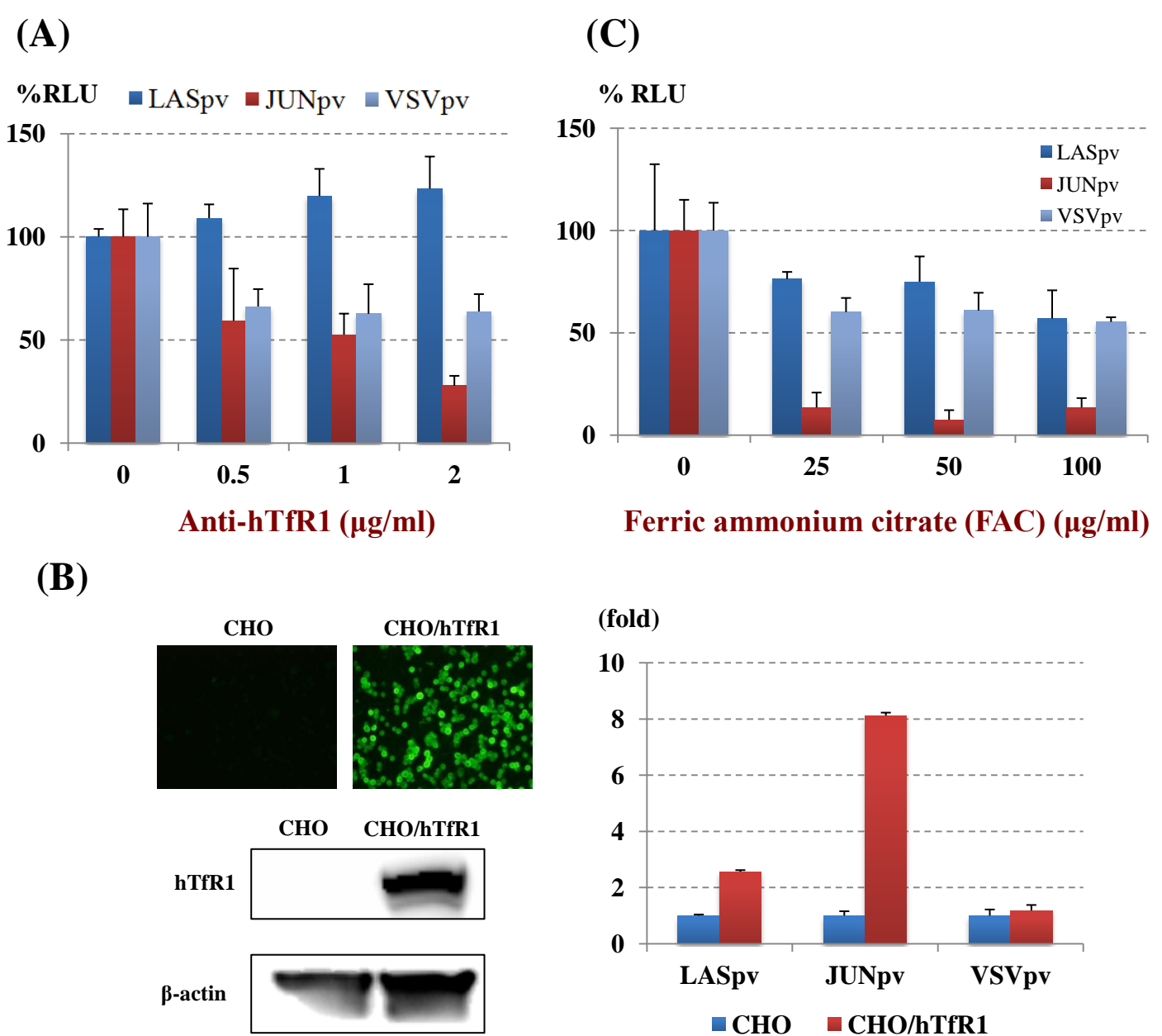**Figure 1-4. Inhibition of infections of LASVpv and JUNVpv by H^+-ATPase inhibitors.**
LASpv, JUNpv or MLVpv were inoculated to Huh7 cells after treatment with various concentrations of bafilomycin A_1 (A), ammonium chloride (B) or chloroquine (C). Luciferase activities were determined at 24 h post-infection. The results shown are from three independent assays, with the error bars representing the standard deviations.
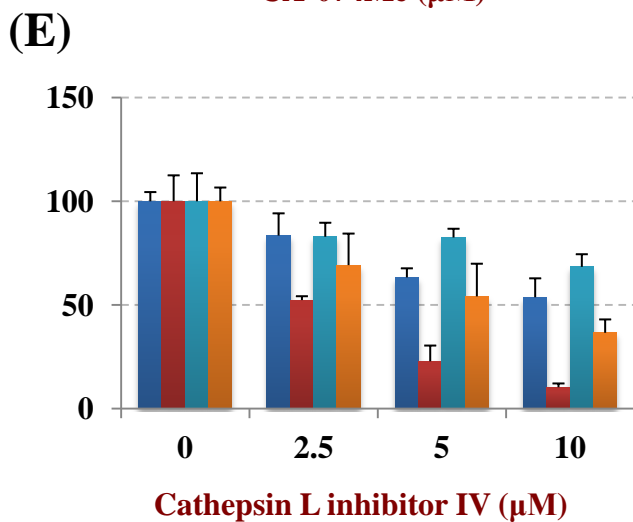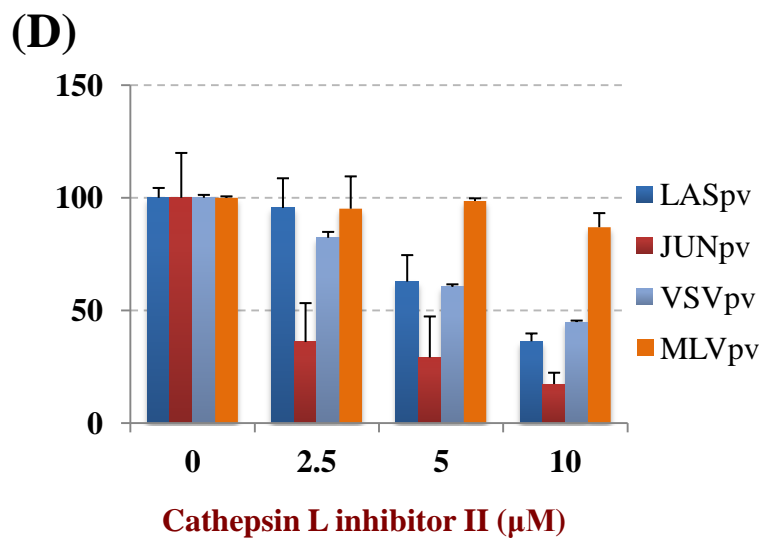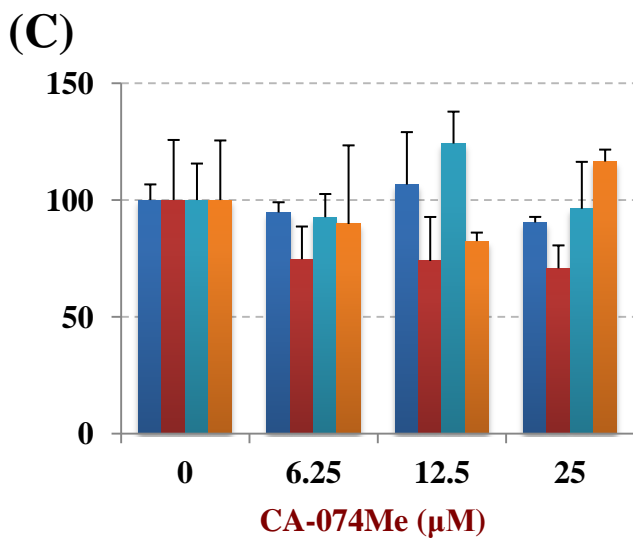
(A)

(B)

Figure 1-5. pH dependence membrane fusion induced by arenavirus GP
(A)Syncytium formation of Huh7 cells transiently expressing LAS GP, JUN GP or VSV-G after treatment with low pH exposure. Huh7 cells were transfected with the plasmids encoding LAS GP, JUN GP or VSV-G. After 24 h post-transfection, the cells were treated with the indicated citrate-phosphate buffer for 2 min. Syncytia formations were determined by microscopic examination. (B) Cell fusion reporter assay for AREV-GP. Huh7 cells transfected with the expression plasmids encoding LAS GP, JUN GP or VSV-G together with a plasmid encoding T7 RNA polymerase were co-cultured with Huh7 cells transfected with a luciferase gene plasmid under the control of the T7 promoter. Cell fusion activity after treatment with the indicated pH exposure for 2 min was determined by the relative luciferase activities (% RLU). The error bars representing the standard deviations of three independent experiments.

(A)

(C)

(B)

Figure 1-6. Involvement of hTfR1 in infection of JUNpv.
(A) Inhibition of LASpv, JUNpv and VSVpv infection by anti-hTfR1 antibody. Huh7 cells were pretreated with various concentrations of anti-hTfR1 antibody for 1 h and inoculated with LASpv, JUNpv or VSVpv, and infectivities were determined at 24 h post-infection by measuring the luciferase activity. (B) Expression of hTfR1 on the CHO cells cell lines constitutively expressing hTfR1 (stable CHO-TfR1 cells) was examined by immunofluorescence assay (upper left panel) or western blotting assay (bottom left panel). CHO or stable CHO-TfR1 cells were infected with LASpv, JUNpv or VSVpv, and infectivities were determined at 24 h post-infection by measuring the luciferase activities. Infectivity of stable CHO-TfR1 cells with each VSV pseudotype was normalized to the infectivity of parental CHO cells. The results shown are from three independent assays, with th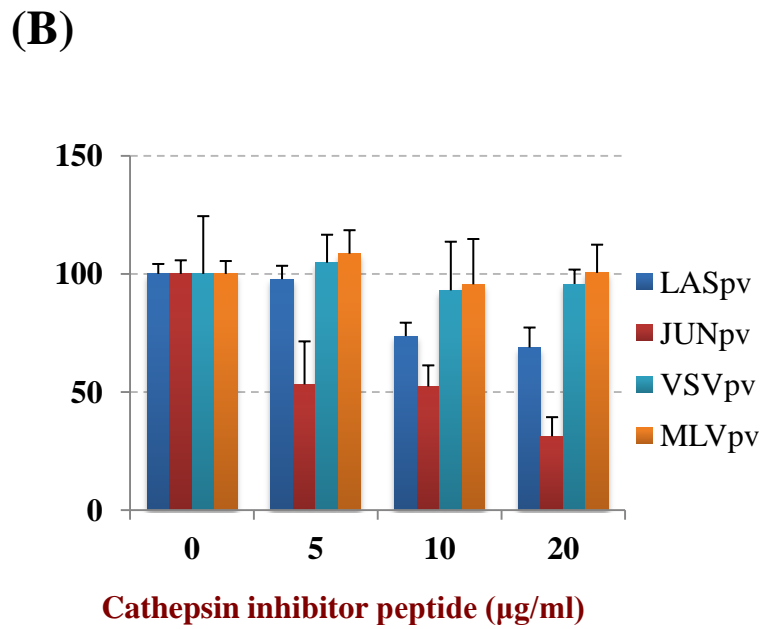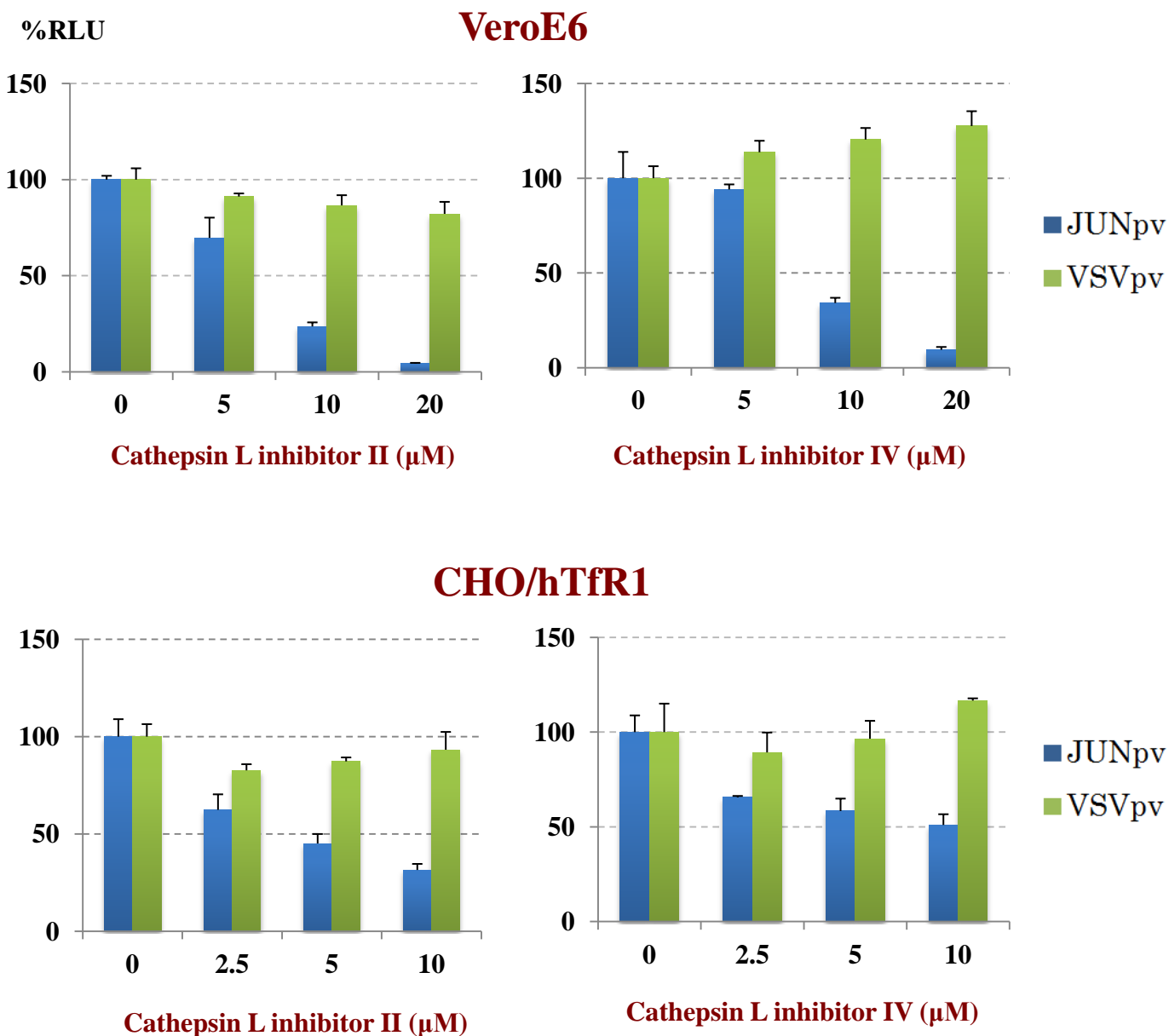e error bars representing the standard deviations. (C) Huh7 cells were pretreated with the indicated concentration of ferric ammonium citrate (FAC), and incubated at 37˚C. After incubation, the cells were inoculated with LASpv, JUNpv or VSVpv. Infectivities were determined by measuring luciferase activity after 24 h of incubation at 37˚C. In each experiment, relative RLU activity with untreated cells was shown with the error bars representing the standard deviations of three independent experiments.

(A)

%RLU

Leupeptin (μg/ml)

(B)

Cathepsin inhibitor peptide (μg/ml)

LASpv
JUNpv
VSVpv
MLVpv

(C)

CA-074Me (μM)

(D)

Cathepsin L inhibitor II (μM)

LASpv
JUNpv
VSVpv
MLVpv

(E)

Cathepsin L inhibitor IV (μM)

43

(F)

VeroE6

Cathepsin L inhibitor II (µM)

Cathepsin L inhibitor IV (µM)

CHO/hTfR1

Cathepsin L inhibitor II (µM)

Cathepsin L inhibitor IV (µM)

Figure 1-7. Involvement of cellular proteases in infection of JUNpv
Huh7 cells were pretreated with various concentrations of protease inhibitors; (A)leupeptin, (B) cathepsin inhibitor peptide, (C) CA-074Me, (D) cathepsin L inhibitor peptide II, or (E) cathepsin L inhibitor peptide IV for 1h at 37˚C, then inoculated with LASpv, JUNpv, VSVpv, or MLVpv, and cultured for 24 h. (F) Vero E6 cells or stable CHO-TfR1 cells were pretreated with cathepsin L inhibitor peptide II or cathepsin L inhibitor peptide IV for 1h at 37˚C, then inoculated with a series of JUNpv or VSVpv and cultured for 24 h. In each experiment, relative RLU activity with untreated cells was shown with the error bars representing the standard deviations of three independent experiments.

Chapter 2

Establishment of serological diagnostic method for Argentine hemorrhagic fever using recombinant antigens

ABSTRACT

JUNV, MACV, GTOV and SABV belong to clade B of New world arenaviruses and are the etiological agents of Argentine hemorrhagic fever (AHF), Bolivian hemorrhagic fever, Venezuelan hemorrhagic fever, and Brazilian hemorrhagic fever, respectively. CHPV was also recently identified to be associated with hemorrhagic fever in Bolivia.

In this study, we have developed a neutralization (NT) assay using a novel vesicular stomatitis virus (VSV) pseudotype bearing Junin virus glycoprotein (JUNV-GP) and the NT has been shown to be equally sensitive and specific in detection of neutralizing antibodies compared to NT using infectious JUNV. Cross-reactivities of antibodies in AHF patients' sera with Machupo, Guanarito, Sabia and Chapare viruses were also analyzed by the NTs using VSV pseudotypes bearing the respective viral GPs, IgG-ELISAs using the respective viral NPs and IFAs using the respective viral NP expressing cells. AHF patients' sera have been shown to cross-react to other clade B arenaviruses in IgG-ELISA and IFA. However, there was no cross-neutralization at all to other arenaviruses causing South American hemorrhagic fever in the NT using VSV-pseudotype, indicating the NT is useful in differential diagnosis among South

American hemorrhagic fever.

INTRODUCTION

AHF is a rodent-borne viral hemorrhagic fever that is endemic in Argentina. The

mortality rate of AHF is estimated to reach 15 to 30 % in untreated case (Enria *et al*.,

2008). Since the introduction of a live attenuated vaccine, Candid #1, in the 1990s, a

constant reduction in the AHF cases was achieved from annual cases of several

hundreds to 3,500 to those of 30 to 50 (Ambrosio *et al*., 2011). However, the

geographic distribution of the endemic region is expanding in the last decades

including the surrounding of Rosario with population of over 1 million, thus about 5

million of humans are considered to be at risk for AHF (Enria *et al*., 2008, Maiztegui

et al., 1986). AHF is caused by JUNV, a member of Tacaribe complex lineage B of the

NW arenaviruses, which include GOTV, SABV, MACV and CHPV, the etiological

agents of Venezuelan, Brazilian, Bolivian and newly identified hemorrhagic fevers in

Bolivia, respectively (Charrel *et al*., 2003, Delgado *et al*., 2008). Arenaviruses are

enveloped and bisegmented RNA viruses. Viral S segment RNA encodes a viral

glycoprotein precursor (GPC) and a nucleocapsid protein (NP), while L segment RNA

encodes an L polymerase and a small RING finger protein (Z) (Meyer *et al*., 2002).

The NP of the lineage B arenaviruses are serologically cross-reactive with each other

in indirect immunofluorescent assay (IFA) and enzyme-linked immunosorbent assay (ELISA) (Sanchez *et al*., 1989, Howard CR. 1986).

For laboratory diagnosis of patients with arenavirus hemorrhagic fevers, detection of viral RNAs and / or viral antigens in the patients' specimens are crucial for rapid diagnosis of patients in the acute phase (Drosten et al., 2002, Jahrling *et al.*, 1985, Niklsson *et al.*, 1984, Olschläger *et al.*, 2010). To detect the viral RNAs in reverse transcription-polymerase chain reaction (RT-PCR), conventional RT-PCRs and TaqMan RT-PCRs were developed (Bockstahler *et al*., 1992, Lozano *et al*., 1993., Lozano *et al*., 1995., Vieth *et al*., 2005). Since the NP is the most abundant protein among the arenavirus structural proteins (Buchmeier *et al*., 1981) and is known to be the most conserved in the same virus species (Bui *et al*., 2007, Gonzalez *et al*., 1996), the antigen-capture ELISA was developed using JUNV NP specific monoclonal antibody (MAb). The antigen-capture ELISA using MAb C6-9 was specific for detection of JUNV NP, while that using MAb C11-12 was capable of detecting JUNV and other pathologic arenaviruses, GUNV, SABV, MACV and CHPV (Nakauchi *et al*., 2009). On the other hand,, JUNV antibodies have been detected by the complement fixation (CF) test and the IFA. Recently, the ELISA has been used for serological diagnosis of AHF and seroepidemiological surveillance of JUNV infection (Garcia *et al*., 1988, Riera *et al*

49

1997, Morales *et al*., 2002), due to its simplicity and high sensitivity. Neutralization test (NT) also has been used for detecting neutralization antibody against JUNV (Ambrosio *et al*., 2006). However, these conventional JUNV based antibody detection systems require handling of live JUNV, which raise safety concerns. Since JUNV is endemic and a live attenuated vaccine for JUNV is approved in Argentina, JUNV is a biosafety level (BSL) 3 pathogen in the country. However, the virus is classified in BSL4 pathogens in the non-endemic countries, thus it is difficult to prepare the ELISA antigens and IF antigens and to conduct NT in laboratories without BSL4 facilities except for Argentina. In this regard, recombinant JUNV NP antigen based IgG-ELISA was developed and shown to be useful for etiologic confirmation of AHF in seroepidemiological studies (Ure *et al*., 2008).

In the chapter 2, I established a novel NT using the replication incompetent VSV pseudotype. The VSV pseudotype based NT has been shown to be useful in differentiating AHF from other arenavirus infections.

MATERIALS AND METHODS

Serum Samples

Seventeen serum samples (#1 to #17) collected in Argentina were used in the study. Fifteen of the 17 sera were collected from 10 AHF patients. Serum samples of #2 to #5, those of #6 and #7, those of #8 and #9 were periodically collected from the same patients, respectively. The sera were used for serological analyses after heat-inactivation at 56°C for 30 min. All the samples were from the biobank at Instituto Nacional de Enfermedades Virales Humanas "Dr. J. I. Maiztegui" (INEVH), which works in concordance with the international and Argentine national regulations, included in the International Ethical Guidelines for Biomedical Research involving human subjects, prepared by the council for International Organizations of Medical Sciences (CIOMS) in collaborating with the World Health Organization (WHO), and particularly, based in the use of the Good Clinical and Laboratory Practices.

Junin virus based neutralization test and IgG-ELISA

NT using JUNV was performed as described previously (Barrera Oro *et al*, 1990). Briefly, JUNV Candid #1 was mixed with serially 2-fold diluted heat-inactivated test

sera, beginning at a dilution of 1 in 5, and incubated for 1 hr at 36˚C, then the

virus-serum mixture was inoculated into Vero cells. Plaque reduction neutralization

titers of the sera were expressed as reciprocals of highest serum dilutions that inhibited

80% plaque formation of JUNV.

IgG-ELISA using JUNV antigen was performed by the method described

previously (Morales *et al*., 2002). In the ELISA, the detergent extracted cell lysates of

JUNV XJCl3 strain infected Vero cells were used as ELISA antigen. The experiments

using infectious JUNV were performed at Instituto Nacional de Enfermedades Virales

Humanas, Argentina (INEVH) in collaboration with Dr. Delia A. Enria, and at

Universidad Nacional de La Plata, Argentina in collaboration with Prof. Victor

Romanowski.

Generation of VSV pseudotype bearing arenavirus GP

The GPC cDNAs of JUNV (MC2 strain) and LASV (Josiah strain) used in the

study was described in the Chapter 1 and the GPC cDNAs of the MACV, GTOV, SABV,

and CHPV were obtained by chemical synthesis (Codon Devices, Cambridge, MA). The

GenBank accession numbers of the nucleotide sequences of JUNV, LASV, MACV,

GTOV, SABV, and CHPV GPC genes are U70799, J04324, NC_005078, AF485258,

NC_006317, and NC_010562, respectively. The cDNAs of the JUNV, MACV, GTOV, SABV, CHPV and LASV GPs were cloned into the expression vector, pKS336 (Saijo *et al.*, 2002). The resulting plasmids were designated as pKS-JUNV-GP, pKS-MACV-GP, pKS-GTOV-GP, pKS-SABV-GP, pKS-CHPV-GP, and pKS-LASV-GP, respectively.

293T cells and Vero E6 cells were maintained in DMEM (Invitrogen) supplemented with 5% fetal bovine serum (FBS) and antibiotics (Kanamycin; GIBCO). 293T cells were transfected with pKS-JUNV-GP and cultured for 24 hr at 37°C in a CO_2 incubator, then the cells were infected with G-complemented (*G) VSVΔG/GFP (*G-VSVΔG/GFP) (Whitt MA, 2010). After absorption for 1 hr, the inoculum was replaced with culture medium and cultured for 24 hr. The culture supernatants were then collected and stored at -80°C until use. The infectious titer (referred to as infectious unit, IU) of the VSV pseudotype (referred to as JUNpv*) was determined on Vero E6 cells by counting numbers of green fluorescent protein (GFP) expressing cells under a fluorescence microscope (BIOREVO BZ-9000, Keyence). VSV pseudotypes bearing GPs of LASV, MACV, SABV, GTNV and CHPV were generated with the same procedures as described above and were designated as LASpv*, MACpv*, SABpv*, GTOpv* and CHPpv*, respectively.

Neutralization test using VSV pseudotypes

The sera were diluted 2-fold from 1 in 80 with DMEM containing 5% FBS, then mixed with 1,000 IU of JUNpv* in the same medium. The mixture was incubated for 1 hr at 37°C and inoculated onto Vero E6 cells seeded on 96-well plates. The numbers of GFP-positive cells were counted under the fluorescence microscope. NT titers of the tested sera were expressed as reciprocals of serum dilutions at which 50% inhibition of the JUNpv* infectivity (NT50) was observed. The values of NT50 were calculated by probit analysis. Serum samples were considered to be negative when less than 50% inhibition of infectivity was observed at a dilution of 1 in 80. All experiments were conducted in triplicate.

NT using MACpv*, SABpv*, GTOpv* and CHPpv* were conducted as the same procedure described above.

Recombinant JUNV-NP based IgG-ELISA

Expression and purification of recombinant JUNV-NP, MACV-NP, GTOV-NP, SABV-NP, CHPV-NP and LASV-NP using the respective recombinant baculoviruses were described previously (Nakauchi *et al*., 2009, Saijo *et al*., 2007). Negative control antigen was prepared using the recombinant baculovirus that lacks the polyhedron gene.

Half of the wells of the ELISA plates (Falcon, NJ, USA) were coated with 100

ng/well of the purified recombinant JUNV-NP (JUNV-rNP) in PBS and the rest of the

wells were coated with the negative control antigen. After washing the plates three times

in PBS containing 0.05% Tween-20 (SIGMA-ALDRICH, MO, USA) (T-PBS), each

well of the plates was incubated with 200μL of T-PBS containing 5% skim milk

(Yukijirushi, Hokkaido, Japan) (MT-PBS) for 1 hr at 37˚C. After washing the plates

three times with T-PBS, the antigen-coated and negative control antigen-coated wells

were inoculated with the AHF patient sera in MT-PBS (100μL/well) at a dilution of 1 in

100, for 1 hr at 37˚C, the plates were washed in T-PBS. Then, each well of the plates

was incubated with a Protein A/G conjugated with horseradish peroxidase at a dilution

of 1 in 1,500 (PIERCE, IL, USA) in MT-PBS for 1 hr at 37˚C. The plates were washed

three times and 100μL of ABTS solution (Roche Diagnostics, Mannheim, Germany)

was added to each well. The plates were incubated for 30 min at room temperature and

optical density (OD) was measured at 405 nm with a reference at 490 nm. The adjusted

ODs for each tested samples were calculated by subtracting the ODs of negative control

antigen coated wells from those of the corresponding JUNV-rNP antigen coated wells.

All experiments were conducted in triplicate. Serum samples were considered to be

negative when average OD value was below 0.2.

Immunofluorescence Assay (IFA)

HeLa cells were transfected with pKS-JUNV-NP (Nakauchi *et al*., 2009) using the FuGENE HD (Roche Diagnostics, Mannheim, Germany) according to the manufacturer's instructions. The transfected cells were selected with 3 μg/mL of blasticidin S-hydrochloride (Invitrogen, CA, USA) in DMEM supplemented with 5% FBS. The selected HeLa cells were dispersed by trypsine-EDTA (Gibco) and washed three times in PBS. Then, the selected HeLa cells were mixed with equal numbers of normal HeLa cells. Mixed cells (10,000 cells /well in PBS) were spotted on multiwell slide glasses (BD biosciences). After the slide glasses were air-dried for 2 hr, the cells were fixed in acetone for 5 min. The fixed slide glasses were used as antigens for IFA specific to JUNV-NP. Similarly, IFA antigens specific to MACV-NP, GTOV-NP, SABV-NP, CHPV-NP and LASV-NP were prepared as described previously (Nakauchi *et al*., 2009, Saijo *et al*., 2007).

The antigen slides were incubated with serially diluted AHF patients' sera under humidified conditions at 37°C for 1 hr. The antigen slides were washed with PBS, then reacted with Goat anti-Human IgG-FITC (Zymax, 81-7111) conjugated with fluorescein isothiocianate (FITC) (Bethyl, TX, USA) at a dilution of 1 in 100 at 37°C for 1 hr. The slides were washed with PBS, mounted with cover glasses and the staining patterns

were examined under a fluorescent microscope with appropriate barrier and excitation filters for FITC visualization. The antibody titer in the IFA was expressed as the reciprocals of the highest dilution showing positive staining. Serum samples were considered to be negative when no positive staining was shown at a dilution of 1 in 20.

Statistical analysis

To evaluate the agrrement between NT using infectious JUNV and that using JUNpv* and the agreement between ELISA using JUNV antigen and that using JUNV-rNP, Spearman's rank correlation coefficient was calculated using Stat Flex software (Artech Co. Ltd., Osaka, Japan).

RESULTS

Detection of neutralization antibodies to JUNV in AHF patients using VSV-JUNV-GP

To examine whether the neutralization antibodies induced in AHF patients neutralize VSV-JUN-GP infection, serum samples periodically collected from an AHF patient (serum #3, #4 and #5) were analyzed by NT using VSV-JUNV-GP. The PRNT titers of the serum samples #3, #4 and #5 using JUNV candid #1 were 160, 640 and 1,280, respectively (Table 2-1). The patient's sera inhibited infection of VSV-JUNV-GP to Vero E6 cells in a dose-dependent manner (Fig. 2-1). Samples were considered NT antibody positive when VSV-JUNV-GP infection was inhibited by 50% or greater as compared to serum-negative control, and the NT titers of the serum samples #3, #4and #5 were calculated to be 200, 400 and 1,500, respectively (Fig. 2-1 and Table 2-1). The results indicated that NT using the VSV pseudotype showed similar sensitivity in detection of NT antibodies using live JUNV. To further validate the sensitivity and specificity of NT using the VSV-JUN-GP, NT titers of all the 17 serum samples were measured by NT using the VSV pseudotype and that using live JUNV (Table 2-1). In NT using live JUNV, we considered samples showing PRNT titers less than 40 were NT

antibody negative. As shown in Table 2-1, fourteen out of the 17 sera were positive by NT using JUNV while 12 of the 14 sera were positive by NT using the VSV pseudotype. Since some antibody-negative human sera showed nonspecific inhibition of VSV pseudotype infection up to a serum dilution of 1 in 40 (data not shown), samples were tested at dilutions of 1 in 80 or higher, with this value set as the cutoff. Neutralizing antibody titer of the serum sample #6 and #10 using VSV pseudotype was 40, thus considered negative. As a result, sensitivity and specificity of NT using the VSV pseudotype compared with that using live JUNV were 12/14 (86%) and 3/3 (100%), respectively (Table 2-2). As shown in Fig. 2-2, scatter diagram describes the correlation between neutralizing antibody titers measured using VSV-JUN-GP and those using live JUNV. There was a significant positive correlation (correlation coefficient, rS=0.870) between the neutralizing titers determined by VSV-JUN-GP and live JUNV.

IFA

IFA using HeLa cells expressing LASV-rNP for detecting LASV specific antibodies in Lassa fever patients has been previously shown (Saijo *et al*, 2007). Thus, JUN-rNP was expressed in HeLa cells by transfecting pKS336-JUNV-NP. As shown in Fig. 2-3, JUNV-rNP antigen was stained by AHF patient serum as fine granules in the

cytoplasm, while any specific staining was not observed by a healthy control serum. As

shown in Table 2-1, twelve out of the 17 sera were positive by the IFA.

Comparison of IgG-ELISA using JUNV antigen and that using JUN-rNP

It has been previously shown that the efficacy of IgG-ELISA using JUN-rNP

(Ure *et al*, 2008). In the present study, antibody titers in the AFH patients' sera were

obtained by both ELISAs and these were compared. Of 12 AHF patients' sera positive

by NT using live JUNV, eleven were positive by both ELISAs, while #11 serum, which

showed NT antibody by both NT assays, was negative by both ELISAs (Table 2-1). The

serum (#11) was also negative by the IFA specific to JUNV-rNP. NT detects

neutralization antibodies on the GP, while ELISA and IFA specific to JUNV-rNP detect

NP antibodies. Thus, the serum #11 is thought to contain antibodies to JUNV GP but not

to NP. The result also indicated the ELISA using JUNV antigen mainly detects

antibodies to JUNV NP. As shown in Table 2-1, sensitivity of the ELISA using JUN-rNP

was calculated to be 100% in comparison to the ELISA using JUNV antigen. As shown

in Fig. 2-4, scatter diagram describes the correlation between the ELISA using JUNV

antigen and that using JUNV-rNP. There was a significant positive correlation

(correlation coefficient, $rS=0.794$) between the antibody titers determined by both

ELISAs.

Cross-reactivity of JUNV specific antibodies in AHF patients' sera with other arenaviruses

Among South American arenaviruses, serological cross-reactions in the CF, IFA were demonstrated (Howard CR. 1986). However, cross-reactivity of JUNV antibodies in AHF patients' sera with other South American arenaviruses causing South American hemorrhagic fever was not fully analyzed. In this study, I have analyzed serological cross-reactions in the ELISA using JUNV-rNP, IFA using HeLa cells expressing JUNV-rNP and NT using the JUNpv* using AHF patients' sera #5, %7 and #9. There was no cross-reaction to other arenaviruses in NT (Table 2-4). By contrast, in the IFA and ELISA specific to JUNV-rNP, all 3 AHF patients' sera showed cross-reactions to MACV, GTOV, SABV and CHPV, except for no cross-reaction to CHPV of the sera #5 and #7 in the IFA (Table 2-5 and Table 2-6). These results indicated that NPs of the pathogenic South American arenaviruses are serologically cross-reactive, while NT is virus species specific.

DISCUSSIONS

Serologic diagnosis of AHF is usually performed with periodically collected serum samples since hospitalization. NT using live JUNV and the ELISA using JUNV antigen were shown to be sensitive in detection of JUNV specific antibody response in the patients (Garcia *et al*, 1988). They showed the IF was less sensitive in detection of JUNV antibody. In the present study, we have developed NT using the novel VSV pseudotype bearing JUNV-GP and showed the NT was similarly sensitive in detection of JUNV specific neutralization antibodies in the AHF patients. In the study, I generated JUNpv* that expresses GFP upon infection so that the pseudotype is suitable for the use of NT compared to JUNpv that expresses lusiferase upon infection and used in the Chapter 1. Fukushi and colleagues previously developed VSV pseudotype based neutralization assay for SARS coronavirus (Fukushi *et al*., 2006). There are some other reports that show VSV pseudotypes bearing viral envelope proteins can be used for NT (Ogino *et al*., 2003, Kaku *et al*., 2012). Since the VSV pseudotype infects the susceptible cells but no progeny infectious virus is produced, NT using the VSV pseudotype can be carried out at lower biosafety level, BSL2. Moreover, the expression of GFP upon the VSV pseudotype is observed in 10 hrs after infection, thus the result of

NT can be obtained within 1 day. In this regard, the NT using the JUNpv* is useful for serologic diagnosis of AHF suspected patients.

In the present study, the IFA using HeLa cells expressing JUNV-rNP was similarly sensitive in detection of JUNV NP antibody in the AFH patients' sera, however, the titers obtained by the IFA was not well correlated. The IFA titers of some sera were similar to the ELISA titers, while some sera such as #5, #10, #12 to #16 showed lower titers in the IFA compared to the ELISA. This suggested that the epitopes of the JUNV NP recognized in the IFA and the ELISA were somewhat different.

The ELISA using the purified recombinant JUN-NP expressed in insect cells using a recombinant baculovirus was previously reported (Ure *et al*, 2008). In the present study, titers in the ELISA using authentic JUNV antigen and that using JUNV-rNP were compared. As a result, both ELISA were comparable in detection of JUNV antibody in the AHF patients' sera, indicating the ELISA using JUNV antigen mainly detects antibodies to the NP.

Among South American arenaviruses, serological cross-reactions in the CF, IFA were previously demonstrated (Howard CR. 1986). In the present study, we have demonstrated that the cross-reactivity of JUNV antibodies in the AHF patients' sera to other pathogenic South American arenaviruses, MACV, GTOV, SABV and CHPV, in
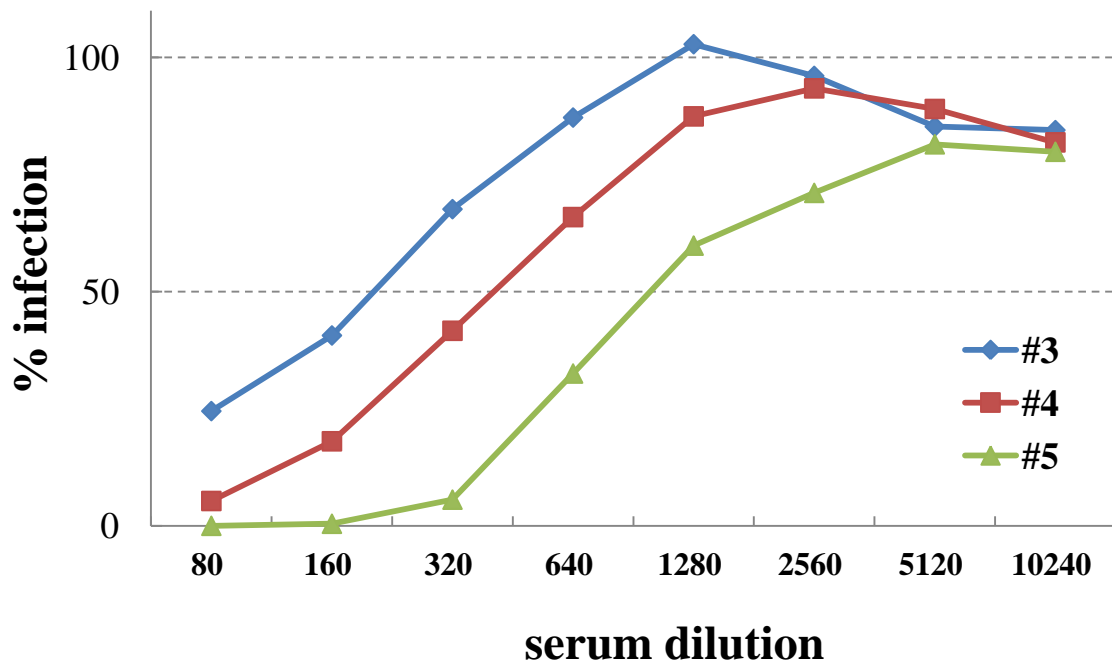
the IFA and ELISA specific to JUNV-rNP. As has been previously shown, a monoclonal antibody (MoAb) to JUNV-NP, C11-12, cross-reacted to MACV, GTOV, SABV and CHPV but not to LASV. The MoAb C11-12 recognized amino acid 12-17 (WTQSLR) region within the NP, which is fully conserved among pathogenic South American arenaviruses but not in LASV (Nakauchi *et al.*, 2009). Similarly, several MoAbs to JUNV NP have been shown to cross-react to other South American arenaviruses (Sanchz *et al*, 1989). A MoAb to Pichinde virus, P3B-3, was also shown to cross-react to variety of arevaviruses including Tacaribe group arenaviruses and old world arevnarisues (Buchmeier *et al*, 1981). Thus the antibodies in the AHF patients might recognize the conserved epitopes on the NP. By contrast, no cross-neutralization to other pathogenic South American arenaviruses was observed in the NT. Thus the NT is thought to be virus species specific even though we could not analyze the cross-reaction in the NT using other South American hemorrhagic fever patients. The NT using the VSV pseudotype is not only useful in serodiagnosis of AHF patients but also in differentiating AHF from other arenavirus infections.

Infectious JUNV has been used for serodiagnosis of AHF, that raised a number of important safety concerns for healthcare professionals. The recombinant protein based serodiagnosis methods developed in this study do not require handling of infectious
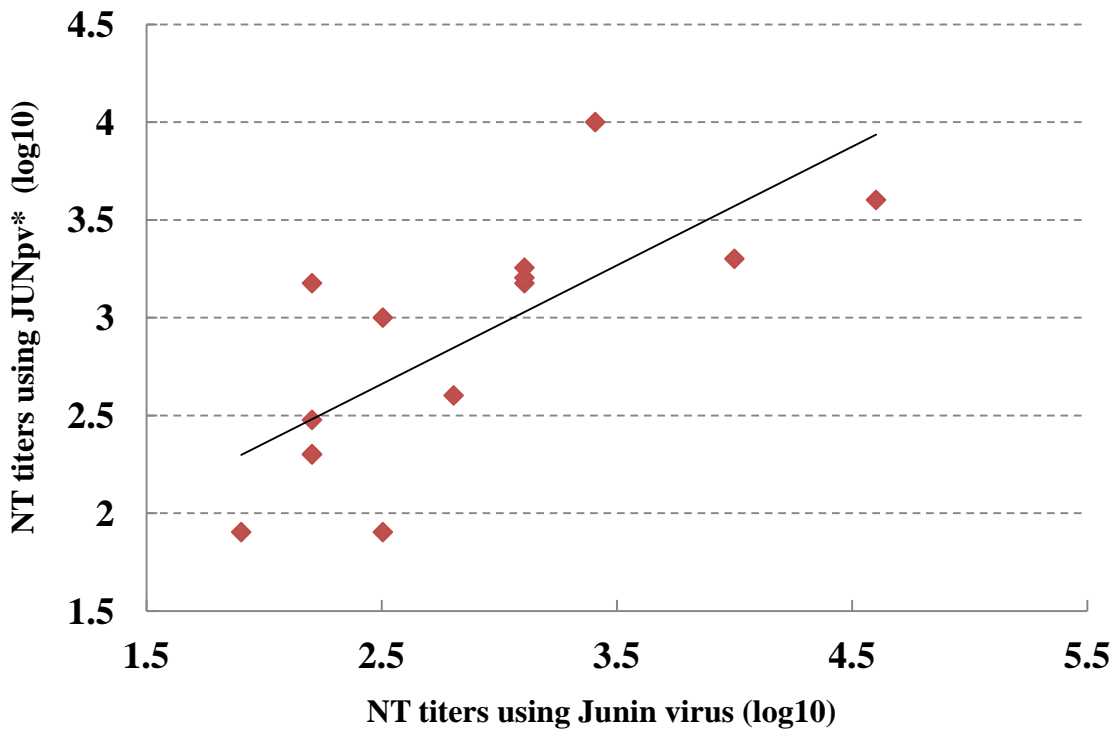
Junin virus, thus the systems will give good solutions for the safety concerns.

In summary, I report here the successful establishment of serodiagnostic systems

for AHF using recombinant JUNV proteins.

Figure 2-1. Detection of neutralization antibodies using JUNpv*.

  Inhibition of JUNpv* infection by periodically collected AHF patient's serum samples (#3, #4, and #5) was shown. JUNpv* was incubated with serially diluted serum samples and infected to VeroE6 cells. The infectivity of the JUNpv was determined by counting number of GFP-expressing cells. Relative infection (% infection) was shown. Reciprocal of dilution showing 50% infection was defined as NT titer of the sample.

Figure 2-2. Correlation between neutralizing antibody titers measured using JUNpv* and those measured using JUNV.
  JUNV neutralizing antibodies in the AHF patients sera were measured by NT using the VSV pseudotype and that using infectious JUNV. NT titers using the pseudotype (on the x-axis in log10 values) and those using JUNV (on the y-axis in log10 values) were plotted. The correlation coefficient between NT titers measured by both methods was $r_S=0.870$.

Figure 2-3. Immunofuorescent assay
Staining patterns of rJUN-NP expressing HeLa cells by sera #5 from AHF patient (A) and a healthy control (B) in IFA.

Figure 2-4. Correlation between ELISA titers measured using JUN-rNP and those using JUNV antigen.
JUNV specific antibodies in the AHF patients sera were measured by ELISA using JUNV-rNP and that using JUNV antigen. ELISA titers using JUNV-rNP (on the x-axis in log10 values) and those using JUNV antigen (on the y-axis in log10 values) were plotted. The correlation coefficient between ELISA titers measured using both antigens was rS=0.794.

Table 2-1. All diagnostic results of each serodiagnostic systems in this study

Serum IDs	JUNV Ag		Recombinant Ag		
	JUNV NT	JUNV ELISA	JUNpv*	rJun-NP IFA	rJun-NP ELISA
#1	20	Negative	<80	<20	<100
#2	5	Negative	<80	<20	<100
#3	160	400	200	160	200
#4	640	400	400	320	400
#5	1280	1600	1500	1280	12800
#6	320	1600	<80	1280	400
#7	160	400	300	5120	3200
#8	160	6400	1500	2560	12800
#9	2560	6400	10000	20480	51200
#10	80	400	<80	20	800
#11	160	Negative	200	<20	<100
#12	1280	6400	1600	640	6400
#13	1280	1600	1800	<20	200
#14	320	1600	1000	320	6400
#15	10000	ND	2000	40	400
#16	40000	ND	4000	20	1600
#17	negative	ND	<80	<20	<100

Gray colored cells indicated positive, and white colored cells indicated negative

Table 2-2 . Comparison of the results of the neutralization assay using JUNpv with those using JUNV

JUNV	JUNpv*		
	Positive	Negative	Total
Positive	12	2	14
Negative	0	3	3
Total	12	5	17

Table 2-3. Comparison of the results of the rJUN-NP based ELISA with JUNV based ELISA

JUNV	rJUN-NP		
	Positive	Negative	Total
Positive	11	0	11
Negative	0	3	3
Total	11	3	14

Table 2-4. Results of neutralization assay using AREpv

Serum IDs	VSV-pseudotypes					
	JUNpv*	MACpv*	GNTpv*	SABpv*	CHPpv*	LASpv*
#5	1,500	<80	<80	<80	<80	<80
#7	300	<80	<80	<80	<80	<80
#9	10,000	<80	<80	<80	<80	<80

Table 2-5. Results of IFA using HeLa cells expressing Arena-NPs

Serum ID	HeLa cells expressing					
	JUN NP	MAC NP	GNT NP	SAB NP	CHP NP	LAS NP
#5	1,280	1,280	640	320	<20	<20
#7	5,120	2,560	320	160	<20	<20
#9	20,480	10,240	5,120	640	160	<20

Table 2-6 . Results of IgG-ELISA using recombinant Arena-NPs

Serum ID	recombinant antigens					
	JUN NP	MAC NP	GNT NP	SAB NP	CHP NP	LAS NP
#5	12,800	12,800	6,400	3,200	800	<100
#7	3,200	1,600	800	400	400	<100
#9	51,200	25,600	12,800	6,400	3,200	200

General Conclusion

Recently, the risks of many infectious diseases have decreased in industrial countries because of the improved sanitary condition, development of anti-microbial drugs and vaccines. However, there are many developing countries in which citizens are suffering from various infectious diseases because of the bad sanitary condition and shortage of medicines. In addition, emerging virus infectious diseases including newly identified arenavirus HF caused by Lujo virus in Republic of South Africa and Zambia (Briese *et al.*, 2009), and by Chapare virus in Bolivia (Delgado *et al.*, 2008), Ebola HF caused by a new type of ebolavirus, Bundibugyo ebola virus, in Uganda (Towner *et al.*, 2008), severe fever with thrombocytopenia syndrome (SFTS) caused by emerging bunyavirus, SFTS virus, in China (Yu *et al.*, 2011) have been recently reported.

As these viruses are extremely pathogenic and difficult in handling, the research concerning to establish their diagnosis and to develop prevention systems have often been impeded. Therefore, development of the safe alternative research tool for these viruses is very important.

In Chapter 1 of this study, I developed VSV pseudotypes bearing envelope protein of Lassa virus or Junin virus and examined their characterization and found that the VSV pseudotypes of arenaviruses mimicked the attachment, internalization and endosomal membrane fusion of infectious arenaviruses. Since many pathogenic

arenaviruses causing VHF in human are classified as the BSL4 pathogens, the VSV pseudotypes of arenaviruses are thought to be quite useful to the further detailed examination on arenavirus entry mechanisms.

In Chapter 2 of this study, I established recombinant antigen-based serological diagnosis systems for AHF. I further analyzed the cross-reactivity of AHF patients' sera with other arenaviruses and found that the arenavirus NP was serologically cross-reactive, while GP antibodies with NT activity are virus species specific. The results found in the chapter indicate that the recombinant antigen-based serological diagnosis systems are useful in serodiagnosis of AHF suspected patients. In addition, NT using the VSV pseudotypes is found to be useful in differential diagnosis among South American hemorrhagic fever.

Through these studies, I have developed safe research tools for arenaviruses, and useful diagnosis methods for AHF. These tools and diagnosis methods can be used almost all research institutes all over the world at BSL2 or lower level. I think the present study could contribute the research and development of treatment and prevention methods for arenavirus HF.

References

Albariño CG, Bergeron E, Erickson BR, Khristova ML, Rollin PE, Nichol ST. 2009.

Efficient reverse genetics generation of infectious junin viruses differing in

glycoprotein processing. J Virol 83(11):5606-5614.

Ambrosio A, Saavedra M, Mariani M, Gamboa G, Maiza A. 2011. Argentine

hemorrhagic fever vaccines. Hum Vaccin 7(6):694-700.

Ambrosio AM, Riera LM, Saavedra MeC, Sabattini MS. 2006. Immune response to

vaccination against Argentine hemorrhagic Fever in an area where different

arenaviruses coexist. Viral Immunol 19(2):196-201.

Barrera Oro JG, McKee KT, Spisso J, Mahlandt BG, Maiztegui JI. 1990. A refined

complement-enhanced neutralization test for detecting antibodies to Junin virus. J

Virol Methods 29(1):71-80.

Barton LL, Hyndman NJ. 2000. Lymphocytic choriomeningitis virus: reemerging

central nervous system pathogen. Pediatrics 105(3):E35.

Bockstahler LE, Carney PG, Bushar G, Sagripanti JL. 1992. Detection of Junin virus

by the polymerase chain reaction. J Virol Methods 39(1-2):231-235.

Borrow P, Oldstone MB. 1994. Mechanism of lymphocytic choriomeningitis virus

   entry into cells. Virology 198(1):1-9.

Bowen MD, Peters CJ, Nichol ST. 1997. Phylogenetic analysis of the Arenaviridae:

   patterns of virus evolution and evidence for cospeciation between arenaviruses and

   their rodent hosts. Mol Phylogenet Evol 8(3):301-316.

Briese T, Paweska JT, McMullan LK, Hutchison SK, Street C, Palacios G, Khristova

   ML, Weyer J, Swanepoel R, Egholm M, Nichol ST, Lipkin WI. 2009. Genetic

   detection and characterization of Lujo virus, a new hemorrhagic fever-associated

   arenavirus from southern Africa. PLoS Pathog 5(5):e1000455.

Buchmeier MJ, Lewicki HA, Tomori O, Oldstone MB. 1981. Monoclonal antibodies to

   lymphocytic choriomeningitis and pichinde viruses: generation, characterization,

   and cross-reactivity with other arenaviruses. Virology 113(1):73-85.

Buckley SM, Casals J. 1970. Lassa fever, a new virus disease of man from West Africa.

   3. Isolation and characterization of the virus. Am J Trop Med Hyg 19(4):680-691.

Bui HH, Botten J, Fusseder N, Pasquetto V, Mothe B, Buchmeier MJ, Sette A. 2007.

   Protein sequence database for pathogenic arenaviruses. Immunome Res 3:1.

Cao W, Henry MD, Borrow P, Yamada H, Elder JH, Ravkov EV, Nichol ST, Compans RW, Campbell KP, Oldstone MB. 1998. Identification of alpha-dystroglycan as a receptor for lymphocytic choriomeningitis virus and Lassa fever virus. Science 282(5396):2079-2081.

Castilla V, Mersich SE. 1996. Low-pH-induced fusion of Vero cells infected with Junin virus. Arch Virol 141(7):1307-1317.

Castilla V, Mersich SE, Candurra NA, Damonte EB. 1994. The entry of Junin virus into Vero cells. Arch Virol 136(3-4):363-374.

Charrel RN, de Lamballerie X. 2003. Arenaviruses other than Lassa virus. Antiviral Res 57(1-2):89-100.

Choe H, Jemielity S, Abraham J, Radoshitzky SR, Farzan M. 2011. Transferrin receptor 1 in the zoonosis and pathogenesis of New World hemorrhagic fever arenaviruses. Curr Opin Microbiol 14(4):476-482.

Delgado S, Erickson BR, Agudo R, Blair PJ, Vallejo E, Albariño CG, Vargas J, Comer JA, Rollin PE, Ksiazek TG, Olson JG, Nichol ST. 2008. Chapare virus, a newly

discovered arenavirus isolated from a fatal hemorrhagic fever case in Bolivia. PLoS
Pathog 4(4):e1000047.

Di Simone C, Buchmeier MJ. 1995. Kinetics and pH dependence of acid-induced
structural changes in the lymphocytic choriomeningitis virus glycoprotein complex.
Virology 209(1):3-9.

Di Simone C, Zandonatti MA, Buchmeier MJ. 1994. Acidic pH triggers LCMV
membrane fusion activity and conformational change in the glycoprotein spike.
Virology 198(2):455-465.

Drosten C, Göttig S, Schilling S, Asper M, Panning M, Schmitz H, Günther S. 2002.
Rapid detection and quantification of RNA of Ebola and Marburg viruses, Lassa
virus, Crimean-Congo hemorrhagic fever virus, Rift Valley fever virus, dengue
virus, and yellow fever virus by real-time reverse transcription-PCR. J Clin
Microbiol 40(7):2323-2330.

Eichler R, Lenz O, Garten W, Strecker T. 2006. The role of single N-glycans in
proteolytic processing and cell surface transport of the Lassa virus glycoprotein
GP-C. Virol J 3:41.

Emonet SF, de la Torre JC, Domingo E, Sevilla N. 2009. Arenavirus genetic diversity

and its biological implications. Infect Genet Evol 9(4):417-429.

Enria DA, Briggiler AM, Sánchez Z. 2008. Treatment of Argentine hemorrhagic fever.

Antiviral Res 78(1):132-139.

Flanagan ML, Oldenburg J, Reignier T, Holt N, Hamilton GA, Martin VK, Cannon PM.

2008. New world clade B arenaviruses can use transferrin receptor 1

(TfR1)-dependent and -independent entry pathways, and glycoproteins from human

pathogenic strains are associated with the use of TfR1. J Virol 82(2):938-948.

Fukushi S, Mizutani T, Saijo M, Kurane I, Taguchi F, Tashiro M, Morikawa S. 2006.

Evaluation of a novel vesicular stomatitis virus pseudotype-based assay for

detection of neutralizing antibody responses to SARS-CoV. J Med Virol

78(12):1509-1512.

Garbutt M, Liebscher R, Wahl-Jensen V, Jones S, Möller P, Wagner R, Volchkov V,

Klenk HD, Feldmann H, Ströher U. 2004. Properties of replication-competent

vesicular stomatitis virus vectors expressing glycoproteins of filoviruses and

arenaviruses. J Virol 78(10):5458-5465.

García Franco S, Ambrosio AM, Feuillade MR, Maiztegui JI. 1988. Evaluation of an

enzyme-linked immunosorbent assay for quantitation of antibodies to Junin virus in

human sera. J Virol Methods 19(3-4):299-305.

Glushakova SE, Lukashevich IS. 1989. Early events in arenavirus replication are

sensitive to lysosomotropic compounds. Arch Virol 104(1-2):157-161.

Gonzalez JP, Bowen MD, Nichol ST, Rico-Hesse R. 1996. Genetic characterization

and phylogeny of Sabiá virus, an emergent pathogen in Brazil. Virology

221(2):318-324.

Harrison LH, Halsey NA, McKee KT, Peters CJ, Barrera Oro JG, Briggiler AM,

Feuillade MR, Maiztegui JI. 1999. Clinical case definitions for Argentine

hemorrhagic fever. Clin Infect Dis 28(5):1091-1094.

Howard CR. in Perspectives in Medical Virology Volume 2: arenaviruses. pp39-41.

Helguera G, Jemielity S, Abraham J, Cordo SM, Martinez MG, Rodríguez JA, Bregni

C, Wang JJ, Farzan M, Penichet ML, Candurra NA, Choe H. 2012. An antibody

recognizing the apical domain of human transferrin receptor 1 efficiently inhibits

the entry of all new world hemorrhagic Fever arenaviruses. J Virol 86(7):4024-4028.

Idemyor V. 2010. Lassa virus infection in Nigeria: clinical perspective overview. J Natl Med Assoc 102(12):1243-1246.

Jahrling PB, Niklasson BS, McCormick JB. 1985. Early diagnosis of human Lassa fever by ELISA detection of antigen and antibody. Lancet 1(8423):250-252.

Kaku Y, Noguchi A, Marsh GA, Barr JA, Okutani A, Hotta K, Bazartseren B, Fukushi S, Broder CC, Yamada A, Inoue S, Wang LF. 2012. Second generation of pseudotype-based serum neutralization assay for Nipah virus antibodies: sensitive and high-throughput analysis utilizing secreted alkaline phosphatase. J Virol Methods 179(1):226-232.

Klewitz C, Klenk HD, ter Meulen J. 2007. Amino acids from both N-terminal hydrophobic regions of the Lassa virus envelope glycoprotein GP-2 are critical for pH-dependent membrane fusion and infectivity. J Gen Virol 88(Pt 8):2320-2328.

Lenz O, ter Meulen J, Klenk HD, Seidah NG, Garten W. 2001. The Lassa virus glycoprotein precursor GP-C is proteolytically processed by subtilase SKI-1/S1P. Proc Natl Acad Sci U S A 98(22):12701-12705.

Lozano ME, Enría D, Maiztegui JI, Grau O, Romanowski V. 1995. Rapid diagnosis of Argentine hemorrhagic fever by reverse transcriptase PCR-based assay. J Clin Microbiol 33(5):1327-1332.

Lozano ME, Ghiringhelli PD, Romanowski V, Grau O. 1993. A simple nucleic acid amplification assay for the rapid detection of Junín virus in whole blood samples. Virus Res 27(1):37-53.

Maiztegui J, Feuillade M, Briggiler A. 1986. Progressive extension of the endemic area and changing incidence of Argentine Hemorrhagic Fever. Med Microbiol Immunol 175(2-3):149-152.

Maiztegui JI, Fernandez NJ, de Damilano AJ. 1979. Efficacy of immune plasma in treatment of Argentine haemorrhagic fever and association between treatment and a late neurological syndrome. Lancet 2(8154):1216-1217.

Marozin S, Altomonte J, Apfel S, Dinh PX, De Toni EN, Rizzani A, Nüssler A, Kato N,
Schmid RM, Pattnaik AK, Ebert O. 2012. Posttranslational modification of
vesicular stomatitis virus glycoprotein, but not JNK inhibition, is the antiviral
mechanism of SP600125. J Virol 86(9):4844-4855.

McCormick JB, Webb PA, Krebs JW, Johnson KM, Smith ES. 1987. A prospective
study of the epidemiology and ecology of Lassa fever. J Infect Dis 155(3):437-444.

Meyer BJ, de la Torre JC, Southern PJ. 2002. Arenaviruses: genomic RNAs,
transcription, and replication. Curr Top Microbiol Immunol 262:139-157.

Moncayo AC, Hice CL, Watts DM, Travassos de Rosa AP, Guzman H, Russell KL,
Calampa C, Gozalo A, Popov VL, Weaver SC, Tesh RB. 2001. Allpahuayo virus: a
newly recognized arenavirus (arenaviridae) from arboreal rice rats (oecomys bicolor
and oecomys paricola) in northeastern peru. Virology 284(2):277-286.

Morales MA, Calderón GE, Riera LM, Ambrosio AM, Enría DA, Sabattini MS. 2002.
Evaluation of an enzyme-linked immunosorbent assay for detection of antibodies to
Junin virus in rodents. J Virol Methods 103(1):57-66.

Nakauchi M, Fukushi S, Saijo M, Mizutani T, Ure AE, Romanowski V, Kurane I, Morikawa S. 2009. Characterization of monoclonal antibodies to Junin virus nucleocapsid protein and application to the diagnosis of hemorrhagic fever caused by South American arenaviruses. Clin Vaccine Immunol 16(8):1132-1138.

Niklasson BS, Jahrling PB, Peters CJ. 1984. Detection of Lassa virus antigens and Lassa virus-specific immunoglobulins G and M by enzyme-linked immunosorbent assay. J Clin Microbiol 20(2):239-244.

Ogbu O, Ajuluchukwu E, Uneke CJ. 2007. Lassa fever in West African sub-region: an overview. J Vector Borne Dis 44(1):1-11.

Ogino M, Ebihara H, Lee BH, Araki K, Lundkvist A, Kawaoka Y, Yoshimatsu K, Arikawa J. 2003. Use of vesicular stomatitis virus pseudotypes bearing hantaan or seoul virus envelope proteins in a rapid and safe neutralization test. Clin Diagn Lab Immunol 10(1):154-160.

Olschläger S, Lelke M, Emmerich P, Panning M, Drosten C, Hass M, Asogun D, Ehichioya D, Omilabu S, Günther S. 2010. Improved detection of Lassa virus by reverse transcription-PCR targeting the 5' region of S RNA. J Clin Microbiol 48(6):2009-2013.

Paessler S, Walker DH. 2012. Pathogenesis of the Viral Hemorrhagic Fevers. Annu
Rev Pathol.

Paweska JT, Sewlall NH, Ksiazek TG, Blumberg LH, Hale MJ, Lipkin WI, Weyer J,
Nichol ST, Rollin PE, McMullan LK, Paddock CD, Briese T, Mnyaluza J, Dinh TH,
Mukonka V, Ching P, Duse A, Richards G, de Jong G, Cohen C, Ikalafeng B,
Mugero C, Asomugha C, Malotle MM, Nteo DM, Misiani E, Swanepoel R, Zaki SR,
Teams OCaI. 2009. Nosocomial outbreak of novel arenavirus infection, southern
Africa. Emerg Infect Dis 15(10):1598-1602.

Radoshitzky SR, Abraham J, Spiropoulou CF, Kuhn JH, Nguyen D, Li W, Nagel J,
Schmidt PJ, Nunberg JH, Andrews NC, Farzan M, Choe H. 2007. Transferrin
receptor 1 is a cellular receptor for New World haemorrhagic fever arenaviruses.
Nature 446(7131):92-96.

Riera LM, Feuillade MR, Saavedra MC, Ambrosio AM. 1997. Evaluation of an
enzyme immunosorbent assay for the diagnosis of Argentine haemorrhagic fever.
Acta Virol 41(6):305-310.

Rojek JM, Lee AM, Nguyen N, Spiropoulou CF, Kunz S. 2008. Site 1 protease is
required for proteolytic processing of the glycoproteins of the South American

hemorrhagic fever viruses Junin, Machupo, and Guanarito. J Virol 82(12):6045-6051.

Rojek JM, Spiropoulou CF, Campbell KP, Kunz S. 2007. Old World and clade C New World arenaviruses mimic the molecular mechanism of receptor recognition used by alpha-dystroglycan's host-derived ligands. J Virol 81(11):5685-5695.

Saijo M, Georges-Courbot MC, Marianneau P, Romanowski V, Fukushi S, Mizutani T, Georges AJ, Kurata T, Kurane I, Morikawa S. 2007. Development of recombinant nucleoprotein-based diagnostic systems for Lassa fever. Clin Vaccine Immunol 14(9):1182-1189.

Saijo M, Qing T, Niikura M, Maeda A, Ikegami T, Sakai K, Prehaud C, Kurane I, Morikawa S. 2002. Immunofluorescence technique using HeLa cells expressing recombinant nucleoprotein for detection of immunoglobulin G antibodies to Crimean-Congo hemorrhagic fever virus. J Clin Microbiol 40(2):372-375.

Sanchez A, Pifat DY, Kenyon RH, Peters CJ, McCormick JB, Kiley MP. 1989. Junin virus monoclonal antibodies: characterization and cross-reactivity with other arenaviruses. J Gen Virol 70 (Pt 5):1125-1132.

Shimojima M, Ströher U, Ebihara H, Feldmann H, Kawaoka Y. 2012. Identification of

cell surface molecules involved in dystroglycan-independent Lassa virus cell entry.

J Virol 86(4):2067-2078.

Smelt SC, Borrow P, Kunz S, Cao W, Tishon A, Lewicki H, Campbell KP, Oldstone

MB. 2001. Differences in affinity of binding of lymphocytic choriomeningitis virus

strains to the cellular receptor alpha-dystroglycan correlate with viral tropism and

disease kinetics. J Virol 75(1):448-457.

Spiro MJ, Spiro RG. 2001. Release of polymannose oligosaccharides from vesicular

stomatitis virus G protein during endoplasmic reticulum-associated degradation.

Glycobiology 11(10):803-811.

Takikawa S, Ishii K, Aizaki H, Suzuki T, Asakura H, Matsuura Y, Miyamura T. 2000.

Cell fusion activity of hepatitis C virus envelope proteins. J Virol

74(11):5066-5074.

Tani H, Komoda Y, Matsuo E, Suzuki K, Hamamoto I, Yamashita T, Moriishi K,

Fujiyama K, Kanto T, Hayashi N, Owsianka A, Patel AH, Whitt MA, Matsuura Y.

2007. Replication-competent recombinant vesicular stomatitis virus encoding

hepatitis C virus envelope proteins. J Virol 81(16):8601-8612.

Tani H, Shiokawa M, Kaname Y, Kambara H, Mori Y, Abe T, Moriishi K, Matsuura Y. 2010. Involvement of ceramide in the propagation of Japanese encephalitis virus. J Virol 84(6):2798-2807.

Towner JS, Sealy TK, Khristova ML, Albariño CG, Conlan S, Reeder SA, Quan PL, Lipkin WI, Downing R, Tappero JW, Okware S, Lutwama J, Bakamutumaho B, Kayiwa J, Comer JA, Rollin PE, Ksiazek TG, Nichol ST. 2008. Newly discovered ebola virus associated with hemorrhagic fever outbreak in Uganda. PLoS Pathog 4(11):e1000212.

Ure AE, Ghiringhelli PD, Possee RD, Morikawa S, Romanowski V. 2008. Argentine hemorrhagic fever diagnostic test based on recombinant Junín virus N protein. J Med Virol 80(12):2127-2133.

Vieth S, Drosten C, Charrel R, Feldmann H, Günther S. 2005. Establishment of conventional and fluorescence resonance energy transfer-based real-time PCR assays for detection of pathogenic New World arenaviruses. J Clin Virol 32(3):229-235.

Ward JH, Kushner JP, Kaplan J. 1982. Regulation of HeLa cell transferrin receptors. J Biol Chem 257(17):10317-10323.

Whitt MA. 2010. Generation of VSV pseudotypes using recombinant ΔG-VSV for

studies on virus entry, identification of entry inhibitors, and immune responses to

vaccines. J Virol Methods 169(2):365-374.

Yu XJ, Liang MF, Zhang SY, Liu Y, Li JD, Sun YL, Zhang L, Zhang QF, Popov VL,

Li C, Qu J, Li Q, Zhang YP, Hai R, Wu W, Wang Q, Zhan FX, Wang XJ, Kan B,

Wang SW, Wan KL, Jing HQ, Lu JX, Yin WW, Zhou H, Guan XH, Liu JF, Bi ZQ,

Liu GH, Ren J, Wang H, Zhao Z, Song JD, He JR, Wan T, Zhang JS, Fu XP, Sun

LN, Dong XP, Feng ZJ, Yang WZ, Hong T, Zhang Y, Walker DH, Wang Y, Li DX.

2011. Fever with thrombocytopenia associated with a novel bunyavirus in China. N

Engl J Med 364(16):1523-1532.

Acknowledgement

Appendix 1

Molecular Cloning and Expression Analysis of Bat Toll-Like Receptors 3, 7 and 9

ABSTRACT

In this study, cDNA of Toll-like receptors (TLR) 3, 7 and 9 were synthesized and completely sequenced. The coding regions of cDNA for bat TLR3, TLR7 and TLR9 were 2,718, 3,150 and 3,090 bp in length, respectively. The open reading frames encoded 905, 1,049 and 1,029 amino acids for TLR3, TLR7 and TLR9, respectively. The nucleotide sequences, predicted amino acid sequences and predicted domain structures of the three bat TLRs had high homology with those of other mammals. In addition, the expression profiles of each TLR in main organs were analyzed. Expression of TLR3 was highest in the liver, whereas the expressions of TLR7 and TLR9 were highest in the spleen.

INTRODUCTION

Infectious diseases transmitted by bats have been increasing recently. These diseases include rabies, Ebola hemorrhagic fever, Nipah virus infection and probably SARS-corona virus infection (Calisher *et al*., 2006, Omatsu *et al*., 2007, Wong *et al*., 2007, Woolhouse *et al*., 2005). In addition, some virus inoculation experiments in bats suggest that many of the bat-associated pathogens cause no clinicopathology in the bats themselves or cause less damage than is seen in other animals (Davis *et al.*, 2005, Middleton *et al.*, 2007, Swanepoel *et al.*, 1996, Williamson *et al.*, 2000). Although many studies on viruses carried in bats are under way, little is known about the emergence of these viruses and their interactions with the host.

The current study is the first analysis of the cDNA sequences of bat Toll-like receptors (TLR) 3, 7 and 9 and their mRNA expressions in various bat organs. TLRs recognize structurally conserved molecules derived from microbes that have breached physical barriers and play a key role in the innate immune system (Akira *et al.*, 2004). Among the TLR classes, TLRs 3, 7, 8 and 9 are involved in virus detection. For example, TLR3 detects double-stranded RNA synthesized during viral genome replication of a single-stranded RNA virus. TLR7 and TLR8 bind single-stranded RNA, and TLR9

recognizes unmethylated cytosine-phosphateguanine motifs common to both bacterial

and viral genomic DNA (Uematsu *et al.*, 2004). In addition, only TLR3, TLR7 and

TLR9 induce type 1 interferon during viral infection (Uematsu *et al.*, 2004).

Materials and Methods

Leschenault's Rousette bats (*Rousettus leschenaulti*) were housed under controlled conditions using an air conditioner and a moisture chamber. The animals were kept in steel cages and fed fruit and water at the same time every day. All experiments were performed in accordance with the Animal Experimentation Guidelines of the University of Tokyo and approved by the Institution Animal Care and Use Committee of the Graduate School of Agricultural and Life Sciences, University of Tokyo.

Fresh spleen samples were collected from bats anesthetized with diethyl ether. The spleens were quickly preserved in RNAlater (Ambion, Austin, TX, U.S.A.) and frozen at $-80{℃}$ until use. Total RNA was isolated from the bat spleen with TRIzol Reagent (Invitrogen, Carlsbad, CA, U.S.A.) according to the manufacturer's protocol. The primary cDNA was synthesized by reverse transcription with Superscript®III reverse transcriptase (Invitrogen) using an Oligo (dT)12–18 primer (Invitrogen), followed by PCR with Thermo-Start® Taq DNA Polymerase (ABgene). In order to clone cDNA from the coding region of bat TLR mRNA, RT-PCR was performed using

primer sets designed from the ortholog sequence data of the equine, swine and feline, which are available in the GenBank nucleotide database. The primers were as follows: TLR3 f1, 5'-AAC TCC ATC CAA AGC TGG AGC CAG AA; TLR3 r1, 5'-GCT ATG TTG TTG TTG CTTA GAT CCA GAA TG; TLR3 f2, 5'- CTG GAT CTA AGC AAC AAC AAC ATA GCC AAC; TLR3 r2, 5'-ACC GAG AA C TCG ATG CAC TGA AAC ATT CCA; TLR7 f1, 5'-CTA GAT GGT TTC CTA AAA CTC TGC CCT GTG; TLR7 r1, 5'-CAT TAT AAC AAC GAG GGC AAT TTC CAC T; TLR7 f2, 5'-AAC TTC TTG GCC AAA GAA ATT GGG GAT GC; TLR7 r2, 5'-TGA GTA ATT CCT TCT GAT TGA AAA TA; TLR7 f3, 5'-ACT GTC CCT GAG AGA TTA TCC AAC TGT TCC; TLR7 r3, 5'-TTG CTA AGC TGT ATG CTC TGG GAA AG; TLR9 f1, 5'-CTG ACG CCT GAG GAC CTG GCC AAT CTG AC; TLR9 r1, 5'-CAG GTG GGC AAA GGA CAC CTT CTT GTG GTA; TLR9 f2, 5'-AGC TGG ACA TGC ATG GCA TCT TCT TCC GCT C; TLR9 r2, 5'-GCC ATT GCT TAG GGC CTT CAG CTG GTT TCC; TLR9 f3, 5'-ACC TGC GCC TCT GCC TGG ATG AGG CCC TCT; and TLR9 r3, 5'-GGT TAT AGA AGT GGC GGT TGT CCC TGG TCA. The amplified products were cloned into plasmids by using a TOPO TA Cloning® Kit (Invitrogen), and the inserts were confirmed by DNA sequencing (Applied Biosystems). To determine the remaining 5'- and 3'-terminal gene sequences, both 5' and 3' methods of rapid amplification of

cDNA ends (RACE) were performed using a 5'-Full RACE Core Set (Takara, Tokyo, Japan). Additional specific primers were designed based on the first decoded sequences to confirm the bat TLR nucleotide sequences. The TLR gene specific primers were as follows: TLR3 F1, 5'-CTC CAC TTA CAA GAC GAG GAA ACT; TLR3 R1, 5'-GTT CTG TAT AGC TGG GTG TTG CT; TLR3 F2, 5'-CC CAG TCT CAT AGA GAA GCT TTG; TLR3 R2, 5'-ATA AGT CCT TGA AGA CCT CTG CTG; TLR3 F3, 5'-TCT TTC TCA TCT CCA TGT CCT TAA C; TLR3 R3, 5'-GAG ACG TAT TTC CAT AGA AGA GAG AG; TLR7 F1, 5'-ATG CTC TGT TCT CTT CAA CCT GAC; TLR7 R1, 5'-TTG GGA AAG ATC TAG TTC CCT AAG; TLR7 F2, 5'-TTA CGT CTA CAT AGC AAC TCC CTT C; TLR7 R2, 5'-CCC AAT TAA AAG ACT TGA GCC C; TLR7 F3, 5'-GGT ATG CCT CCA AAT CTA AAG ACT C; TLR7 R3, 5'-GAA CAT TCT TGG TGA GAC ATC TTT G; TLR9 F1, 5'-ACT CCC TGT CAT GGG CCC TTG CCA TGG TGC; TLR9 R1, 5'-AGT TCA TCT GCA GAC TCA GGT TG; TLR9 F2,5'-CAA ACT CAA CCT GTC CTT CAA TTA C; TLR9 R2,5'-ATT GAG CTG CCG CAG ATT CCT; TLR9 F3, 5'-CTG CTG AAG GCC CTG ACC AAC; and TLR9 R3, 5'-GGC TGT CCG CCG TGC TAT TC. The lengths of the PCR products were 891, 1,054, 1,276, 1,021, 1,198, 1,222, 1,214, 1,177 and 1,049 bp, respectively. Sequence analysis was conducted using an ABI 3130/3130xl Genetic Analyzer (ABI). The cDNA sequences of

bat TLR3, TLR7 and TLR9 were deposited in the GenBank database (Accession numbers: AB_472355, AB_472356 and AB_472357). The coding regions of cDNA for TLR3, TLR7 and TLR9 were 2,718, 3,150 and 3,090 bp in length, with open reading frames encoding 905, 1,049 and 1,029 amino acids, respectively. The sequences of the nucleotides and their predicted amino acids share very high homology to the TLRs of other mammals. Bat TLR3, TLR7 and TLR9 had 85.5 to 89.7%, 88.2 to 90.5% and 80.6 to 82.4% sequence homology, respectively, with other mammals. The predicted amino acid sequences of TLR3, TLR7 and TLR9 were 82.8 to 88.5%, 85.7 to 88.0% and 74.3 to 7.2% homologous with those of other mammals, respectively (Table 1). Like other mammalian TLRs (Chang *et al.,* 2008, Sang *et al.,* 2008, Zhang *et al.*, 2008, Zhang *et al.*, 2008), bat TLR3, TLR7 and TLR9 mRNA nucleotide and predicted amino acid sequences showed high similarities to those of other mammalian orthologs. The phylogenic tree generated by comparing bat TLR amino acid sequences and those of other animals showed that bat TLRs are closely related to equine and carnivore TLRs (data not shown), which supports the findings of a previous study (Nishihara *et al*., 2006). Nucleotide and predicted amino acid sequences were analyzed by GENETYX-WIN (Ver 4.0, Software Development Co., Ltd., Tokyo, Japan). The accession numbers of the nucleotide data used for homology analysis were as follows:

TLR3, NM_001081798, XM_540020, NM_001008664, NM_003265; TLR7, NM_001081771, NM_001048124, NM_001033761, NM_016562; TLR9, NM_001081790, NM_001002998, NM_183081, NM_017442. Bat TLR3, TLR7 and TLR9 domain structures were compared with those of other mammalian species orthologs using the SMART (Schults *et al*., 1998) and NCBI BLAST programs (http://blast.ncbi.nlm.nih.gov/Blast.cgi). The results showed that bat TLR3, TLR7 and TLR9 have highly conserved leucinerich repeat (LRR) and Toll/Interleukin-1 receptor (TIR) domains that play critical roles in innate and acquired immunity (Bell *et al*., 2003, Bowie *et al*., 2000) (data not shown).

In addition, semi-quantitative RT-PCR was performed to assess the mRNA expression ratios of TLR3, TLR7 and TLR9 in various organs. Eight tissues or organs (kidney, liver, spleen, brain, ovary, small intestine, lung and heart) were obtained from young female bats (n=5). The respective procedures described above were used to process each organ and synthesize the template cDNA used in the semiquantitative RT-PCR. The expression of beta-actin mRNA was used as an internal control. The primers used in semiquantitative RT-PCR were as follows: TLR3 quantitate F, 5'-AGT TGA CTC AAA TAC CTG ACG ACC; TLR3 quantitate R, 5'-CAA GTT CTT CAC

GGC TTA GTA CG; TLR7 quantitate F, 5'-CAA AGA GAC TCC TTC TTC CTT GAG;

TLR7 quantitate R, 5'-CTA AGA GAT TCA CTC TCC ATG GTC C; TLR9 quantitate F,

5'-CTA CTA CAA GAA CCC GTG CGA C; TLR9 quantitate R, 5'-GTA CAG AAA

GTT CTC ACT CAG GTC C; beta-actin F, 5'-ATT GTG CGT GAC ATC AAG GAG

AAG; and beta-actin R, 5'-ATT CCT GCT TGC TGA TCC ACA TCT. PCR cycles were

conditioned in which growth curves of all organs PCR products run on mid-logarithmic

phase. The PCR products were analyzed in 2% agarose gel, and DNA band intensities

were quantified using the Scion Image software (Scion Corporation, Frederick, ML,

U.S.A.).

RESULTS AND DISCUSSIONS

The expression of bat TLR mRNA varied in the organs. For TLR3, the expression was greatest in the liver, less but fairly equivalent in the kidney, spleen, ovary, intestine and lung and low in the brain and heart (Fig. 1A). In contrast, the expressions of TLR7 and TLR9 were greatest in the spleen. The expressions of both of these TLRs were fairly equivalent in the kidney, liver and ovary and weak in the brain and heart. TLR7, unlike TLR9, had rather high expression in the intestine and lung (Figs. 1B and 1C). These results may reflect the characteristics of the bat immune system. In general, TLR3, TLR7 and TLR9 are highly expressed on endosomes of dendritic cells, and the TLR profiles of these cells are dependent on the cell subtype. For example, in humans and macaques, plasmacytoid dendritic cells, myeloid dendritic cells and monocyte-derived dendritic cells express TLR7 and TLR9, TLR3, TLR7 and TLR9, and TLR3 only, respectively (Ketlov *et al.*, 2008). Therefore, TLR expression in distinct organs is likely dependent on the number of dendritic cells harboring each TLR. Magnetic cell sorting methods (MACS) or fluorescence-activated cell sorting analysis are needed to the delineate cellular distribution of bat TLR3, TLR7 and TLR9, and to analyze detailed features of the bat immune system.

Figure 1. Comparison of TLR/b-actin copy number ratios among organs [(A) TLR3, (B) TLR7, (C) TLR9]. Each ratio was standardized to the ratio measured in the kidney. Vertical lines on the bar graphs indicate the standard deviation.

Table 1. CDS length of the TLR cDNA and sequence similarities

	CDS lengths (bp)	Nucleotides (%)	Amino acids (%)
(A) TLR3			
Chiroptera	2,718	–	–
Equine	2,715	89.7	88.5
Canine	2,718	88.6	85.9
Bovine	2,715	85.5	82.8
Human	2,715	86.6	84
(B) TLR4			
Chiroptera	3,150	–	–
Equine	3,153	90.5	87.9
Canine	3,153	88.2	88
Bovine	3,177	88.7	87
Human	3,150	88.2	85.7
(C) TLR9			
Chiroptera	3,090	–	–
Equine	3,096	82.3	77.2
Canine	3,093	82.4	76.6
Bovine	3,090	81.6	75.6
Human	3,099	80.6	74.3

REFERENCES

Akira S, Takeda K. 2004. Toll-like receptor signalling. Nat Rev Immunol

4(7):499-511.

Bell JK, Mullen GE, Leifer CA, Mazzoni A, Davies DR, Segal DM. 2003.

Leucine-rich repeats and pathogen recognition in Toll-like receptors. Trends

Immunol 24(10):528-533.

Bowie A, O'Neill LA. 2000. The interleukin-1 receptor/Toll-like receptor superfamily:

signal generators for pro-inflammatory interleukins and microbial products. J

Leukoc Biol 67(4):508-514.

Calisher CH, Childs JE, Field HE, Holmes KV, Schountz T. 2006. Bats: important

reservoir hosts of emerging viruses. Clin Microbiol Rev 19(3):531-545.

Chang JS, Russell GC, Jann O, Glass EJ, Werling D, Haig DM. 2009. Molecular

cloning and characterization of Toll-like receptors 1-10 in sheep. Vet Immunol

Immunopathol 127(1-2):94-105.

Davis A, Bunning M, Gordy P, Panella N, Blitvich B, Bowen R. 2005. Experimental
and natural infection of North American bats with West Nile virus. Am J Trop
Med Hyg 73(2):467-469.

Ketloy C, Engering A, Srichairatanakul U, Limsalakpetch A, Yongvanitchit K,
Pichyangkul S, Ruxrungtham K. 2008. Expression and function of Toll-like
receptors on dendritic cells and other antigen presenting cells from non-human
primates. Vet Immunol Immunopathol 125(1-2):18-30.

Middleton DJ, Morrissy CJ, van der Heide BM, Russell GM, Braun MA, Westbury HA,
Halpin K, Daniels PW. 2007. Experimental Nipah virus infection in pteropid
bats (Pteropus poliocephalus). J Comp Pathol 136(4):266-272.

Nishihara H, Hasegawa M, Okada N. 2006. Pegasoferae, an unexpected mammalian
clade revealed by tracking ancient retroposon insertions. Proc Natl Acad Sci U
S A 103(26):9929-9934.

Omatsu T, Watanabe S, Akashi H, Yoshikawa Y. 2007. Biological characters of bats in
relation to natural reservoir of emerging viruses. Comp Immunol Microbiol
Infect Dis 30(5-6):357-374.

Sang Y, Yang J, Ross CR, Rowland RR, Blecha F. 2008. Molecular identification and functional expression of porcine Toll-like receptor (TLR) 3 and TLR7. Vet Immunol Immunopathol 125(1-2):162-167.

Schultz J, Milpetz F, Bork P, Ponting CP. 1998. SMART, a simple modular architecture research tool: identification of signaling domains. Proc Natl Acad Sci U S A 95(11):5857-5864.

Swanepoel R, Leman PA, Burt FJ, Zachariades NA, Braack LE, Ksiazek TG, Rollin PE, Zaki SR, Peters CJ. 1996. Experimental inoculation of plants and animals with Ebola virus. Emerg Infect Dis 2(4):321-325.

Uematsu S, Akira S. 2004. [TLR family and viral infection]. Uirusu 54(2):145-151.

Williamson MM, Hooper PT, Selleck PW, Westbury HA, Slocombe RF. 2000. Experimental hendra virus infectionin pregnant guinea-pigs and fruit Bats (Pteropus poliocephalus). J Comp Pathol 122(2-3):201-207.

Wong S, Lau S, Woo P, Yuen KY. 2007. Bats as a continuing source of emerging infections in humans. Rev Med Virol 17(2):67-91.

Woolhouse ME, Gowtage-Sequeria S. 2005. Host range and emerging and reemerging

pathogens. Emerg Infect Dis 11(12):1842-1847.

Zhang Y, Guo Y, Lv K, Wang K, Sun S. 2008a. Molecular cloning and functional

characterization of porcine toll-like receptor 7 involved in recognition of

single-stranded RNA virus/ssRNA. Mol Immunol 45(4):1184-1190.

Zhang YW, Davis EG, Blecha F, Wilkerson MJ. 2008b. Molecular cloning and

characterization of equine Toll-like receptor 9. Vet Immunol Immunopathol

124(3-4):209-219.

Appendix 2

Molecular Cloning and Sequencing of the cDNAs Encoding the Bat Interleukin (IL)-2, IL-4, IL-6, IL-10, IL-12p40, and Tumor Necrosis Factor-Alpha

ABSTRACT

This is the first report on the cDNA sequences of bat interleukin (IL)-2, IL-4, IL-6, IL-10, IL-12 p40, and tumor necrosis factor (TNF)-α. The cDNAs of bat IL-2, IL-4, IL-6, IL-10, IL-12 p40, and TNF-α comprise 459, 405, 624, 537, 990, and 699 base pairs respectively. Moreover, each of the cDNAs of bat IL-2, IL-4, IL-6, IL-10, IL-12 p40, and TNF-α contain a single open reading frames encoding 152, 134, 207, 178, 329, and 232 amino acids, respectively. The comparison of bat cytokines with Perrissodactyla (horse), Carnivora (dog and cat), and Cetartiodactyla (cattle and pig) orthologs revealed a high degree of homology. Although the N-terminal amino acids and cysteine residues are highly conserved in each mature cytokine, the deduced N-linked glycosylation sites vary across species.

INTRODUCTION

Recently, there has been an increase in the incidence of infectious diseases originating from bats, such as rabies, Ebola virus, Nipah virus, and most likely severe acute respiratory syndrome (SARS) coronavirus (Calisher *et al*., 2006, Omatsu *et al*., 2007, Woolhouse *et al*., 2005). In addition, several studies involving viral inoculations in bats suggest that some bat-associated pathogens cause less clinicopathological damage in this species, or have no effect, compared to other species (Davis *et al*., 2005, Middleton *et al*., 2007, Swanepoel *et al*., 1996, Williamson *et al*., 2000). These findings imply that the cell-mediated immune responses of bats to viruses agents are different from those of other species. Although studies on fruit bats have revealed well-developed immune systems (Paul and Chakravarty, 1986), lower levels of agglutinating, hemagglutinating, and complement-fixing antibodies are produced in response to various antigens in fruit bats than in conventional laboratory animals (Hatten *et al*., 1968). Furtherand, the peak of primary antibody response after antigenic challenge is delayed in fruit bats (Chakraborty *et al*., 1984). Additionally, the activation of T lymphocytes is significantly delayed in bats as compared to in mice (Chakravorty *et al*., 1984, Chakravarty *et al*., 1987). In the present study, we analyzed the cDNA sequences

of bat Th1 (IL-2, and IL-12 p40) cytokines, Th2 (IL-4, IL-6, and IL-10) cytokines, and

tumor necrosis factor (TNF)-α that was selected as the representative inflammatory

cytokines. These cytokines have major roles in inflammation, and both cellular and

humoral immunity. Th1 cells have a key role in the cellular immune response to viruses

and other intracellular pathogens as well as in the elimination of cancer cells and

stimulation of delayed-type hypersensitivity (DTH). On the other hand, Th2 cells drive

humoral immunity and upregulate antibody production in order to neutralize

extracellular organisms (Kidd *et al*., 2003).

MATERIALS AND METHODS

Leschenault's Rousette bats (*Rousettus leschenaulti*) were maintained under controlled conditions using an air conditioner and moisture chamber. The animals were kept in steel cages, and fed fruit and water at the same time everyday. All experiments were performed in accordance with the Animal Experimentation Guidelines of the University of Tokyo, and were approved by the Institutional Animal Care and Use Committee of the Graduate School of Agricultural and Life Sciences, The University of Tokyo.

Fresh spleen samples were collected from Leschenault's Rousette bats (*Rousettus leschenaulti*) under anesthesia with diethylether. The spleen was preserved in RNAlater (Ambion, Austin, TX, U.S.A.) and frozen at −80°C. Total RNA was isolated from bat spleen with TRIzol Reagent (Invitrogen, Carlsbad, CA, U.S.A.), according to the manufacturer's protocol. Primary cDNAs were synthesized by reverse transcription with Superscript®III reverse transcriptase (Invitrogen) using an Oligo (dT)12–18 primer (Invitrogen), followed by PCR with Thermo-Start® Taq DNA Polymerase (ABgene, Epson, UK). To obtain cDNA clones of the middle region of the mRNAs of

bat cytokines, reverse transcriptase-polymerase chain reaction (RT-PCR) was performed using primer sets that are designed from the ortholog sequence data of horse, pig, and cat available on the GenBank database. The primers used for amplifying DNA fragments are described in Table 1. The amplified products were cloned into plasmids using a TOPO TA Cloning® Kit (Invitrogen), and to validate the sequences, 5 clones obtained for each sample were confirmed by DNA sequencing analysis using the ABI 3130/3130xl Genetic Analyzer (Applied Biosystems, Foster City, CA, U.S.A.). To determine the remaining 5'- and 3'-terminal gene sequences, both 5'-rapid amplification of cDNA ends (RACE) and 3'- RACE were performed using a 5'-full RACE core set (TaKaRa, Tokyo, Japan). To confirm the decoded bat interleukin nucleotide sequences, additional specific primers were designed on the basis of the first decoded sequences, and direct sequencing was carried out. The gene-specific primers are described in Table 2. KOD FX DNA polymerase (Toyobo, Osaka, Japan) was used for high-fidelity PCR amplification.

RESULTS AND DISCUSSIONS

The complete nucleotide sequences encoding bat IL-2, IL-4, IL-6, IL-10, IL-12 p40, and TNF-α comprised 459, 405, 624, 537, 990, and 699 base pairs, respectively, and the deduced amino acid sequences comprisedmade 152, 134, 207, 178, 329, and 232 amino acid residues, respectively. The cDNA sequences of IL-2, IL-4, IL-6, IL-10, IL-12 p40, and TNF-α were deposited in the GenBank database (Accession numbers: AB472358, AB472359, AB472360, AB472361, AB472362, and AB472363).

The nucleotide and amino acid sequences were analyzed using the Genetyx-Win software (version 4.0; Software Development Co., Tokyo, Japan). The SignalP program (http://www.expasy.org) was used to predict the position of the N-terminal amino acids of mature proteins. The accession numbers of nucleotide data that were used for homology analysis are described in Table 3. The sequence homology of the nucleotide and amino acid sequences of bat cytokines with other mammalian cytokine orthologs is described in Table 4.

The alignment of the deduced amino acid sequences of bat, horse, dog, cat,

cattle, pig, and human cytokines is described in Figs. 1A-1F. We found 4 conserved cysteine residues (positions 29, 31, 144, and 176) in bat TNF-α. In the TNF-α amino acid sequence, we found 6 amino acid residues (indicated by a rhomboid) involved in interactions at the TNF-α receptor binding site (Hymowitz *et al.*, 2000, Lam *et al.*, 2001]. Of these 6 amino acids in the bat, the Asp164 residue differed from that in other species. More research is required to determine whether this difference affects species-specific affinity of TNF-α for its receptor. In the bat, IL-2 contains 4 conserved cysteine residues (positions 9, 77, 124, and 144) and 1 potential N-linked glycosylation site (positions 109–111). Although the overall amino acid sequence homology was not high, the cysteine residues in IL-2 were highly conserved in the bat and other mammalian species. On the other hand, the N-linked glycosyilation site, which modulates the function of the mature IL-2 protein, was found to be conserved in the bat when compared to that in the horse, dog, cat, and pig; however, N-linked glycosylation sites in the putative IL-2 in cattle and humans are not found at the same sites as in the bat. After post-translational processing, Ala21 was deduced to be the first amino acid residue in the mature IL-2 protein at the N-terminal region. In the bat, IL-12 p40 contained 9 conserved cysteine residues (at positions 50, 90, 131, 142, 170, 194, 200, 301, and 328) and 3 predicted N-linked glycosylation sites (at positions 125–127,

135–137, and 223–225). Consistent with the results of a previous study, we found that the cysteine residues were entirely conserved among species (Odbileg *et al*., 2004). Ile23 is at the putative N-terminus of the mature protein. Bat IL-4 has 5 conserved cysteine residues (at positions 13, 17, 48, 70, and 106) and 2 potential N-linked glycosylation sites (at positions 20–22 and 97–99). Although cysteine residues in IL-4 are highly conserved across species, another study (Odbileg *et al*., 2005) has reported that other mammals have an additional conserved cysteine residue at position 134 (indicated by a double circle in Fig. 1D). For IL-4, Arg25 is at the putative Nterminus of the mature protein. Bat IL-6 has 4 conserved cysteine residues (at positions 70, 76, 99, and 109) and 2 potential N-linked glycosylation sites (at positions 49–51 and 167–169). Although the cysteine residues were entirely conserved, the N-linked glycosylation sites in IL-6 may or may not be present depending on species. For IL-6, Pro27 is at the putative N-terminus of the mature protein. Bat IL-10 has 6 conserved cysteine residues (at positions 8, 9, 30, 80, 126, and 132) and 3 predicted N-linked glycosylation sites (positions 67–69, 100–102, and 134–136). A very high degree of sequence homology was observed in the amino acid sequence of bat IL-10 and IL-10 of other species, and the positions of cysteine residues were highly conserved in IL-10. However, the presence of additional N-linked glycosylation sites (Asn100-Ser102), which are absent
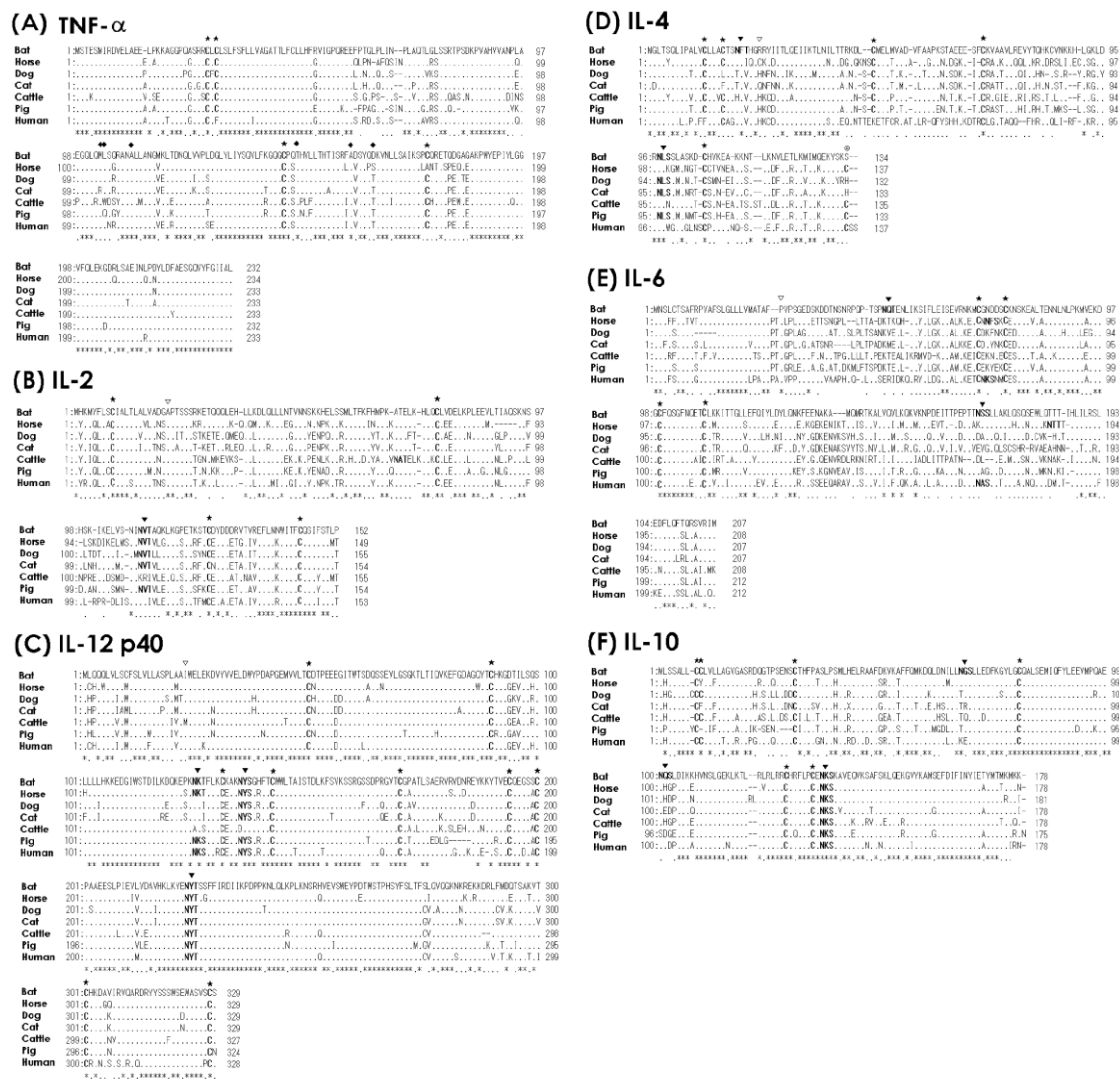
in other mammalian species, may affect the function of bat IL-10. For IL-10, Ser19 is at the putative N-terminus of the mature protein.

In this study, the cDNA sequences of bat cytokines were analyzed. Overall, the comparison of bat cytokines with Perrissodactyla (horse), Carnivora (dog and cat), and Cetartiodactyla (cattle and pig) orthologs revealed a higher degree of homology in terms of the nucleotide and deduced amino acid sequences (Table 4). This is consistent with previous reports that conducted retroposon insertion analysis for examining phylogenetic relationships between organisms of almost all mammalian orders (Nishihara *et al*., 2006). In addition, cysteine residues and N-terminus amino acids of mature cytokines are highly conserved among species (Hirano *et al*., 1986, Taniguchi *et al*., 1983, Vieira *et al*., 1991, Wolf *et al*., 1991, Yokota *et al*., 1986). However, N-linked glycosylation sites vary to some extent inposition and number. These results suggest that although the 3-D conformation of each cytokine is conserved among species, the glycosylation-related functions of each cytokine differ among species. Further research on different species-specific functions of each cytokine is needed to understand the characterization of immune systems in each animal.

The nucleotide sequence data obtained in this study will be very useful for future studies on the bat immune system. In particular, these data coupled with real-time RT-PCR for the quantification of the mRNA of bat cytokines will facilitate kinetic analysis of the cytokines. This is likely to be an excellent method for analysis of the immune system in wild animals, because a specific enzyme-linked immunosorbent assay (ELISA) systems for cytokine analysis across species is unavailable, and such a system would most likely take a long time to develop.

Further research on the bat immune system and infectious diseases originating from bats may provide key insights as to how bats act as natural reservoirs of infectious diseases. Further studies are needed to characterize the bat immune system and to understand the interactions of viruses and other pathogenic microbes with the bat immune system.

(A) TNF-α

(B) IL-2

(C) IL-12 p40

(D) IL-4

(E) IL-6

(F) IL-10

Figure 1. Alignment of the deduced amino acid sequences of bat, horse, dog, cat, cattle, pig, and human cytokines ([A] TNF-α, [B] IL-2,[C] IL-12p40, [D] IL-4, [E] IL-6, and [F] IL-10). Identical amino acid residues are indicated by an asterisk (*) and almost identical amino acid residues are indicated by a dot (.). A black star indicates conserved cysteine residues, and a black arrowhead indicates a potential N-linked glycosylation site. White arrowheads indicate the amino acid terminus of the mature proteins. Amino acids involved in binding TNF-α receptors are indicated by a rhomboid. In Fig. 1D (IL-4), a double circle indicates a predicted substitution of a cysteine residue.

Table 1. Primers used for amplifying the DNA fragments of each Cytokines

Primer name	Sequence(5'–3')
TNF-α F1	AAGCATGATCCGAGATGTGGAGCTGGC
TNF-α R1	CTTCTCCAGCTGGAAGACTCCTCCCAGGTA
IL-2 F1	CTTGCACTTGTCGCAAACAGTGCACCTA
IL-2 R1	GCTTTGAGGTAAACCTAGCACTTCCTC
IL-4 F1	ACTAGCATGTACCAGCAACT
IL-4 R1	TTGGCTTCATTCACAGTACAGC
IL-6 F1	GGATGCTTCCAATCTGGGTTCAATCAGG
IL-6 R1	TGCCCAGTGGACAGGTTTCTGACCAGA
IL-10 F1	CCACATGCTCCATGAGCTCCGAG
IL-10 R1	GATGAAGATGTCAAACTCACTCATGGC
IL-12p40 F1	GGCTCTGGTAAAACTCTGACCATCCAAGTC
IL-12p40 R1	GAACCTAACTGCAGGACACAGATGCCCA

Table 2. Primers used for confirming the decoded sequences

Primer name	Length of PCR product(bp)	Sequence(5'–3')
TNF-α F	898	CAGACAACACAGACCCGGAGAAGCA
TNF-α R		CTAATTCCCTTTCTGAAGAGGATGAG
IL-2 F	569	AGTATAAATTGCTCCTCTTGTTTG
IL-2 R		TAGCCTGATACATTTTAAGTGGGAG
IL-4 F	419	GATCTATTAATGGGTCTCACCTC
IL-4 R		CAGCTTCAACTCTTTGAGTATTTCTC
IL-6 F	762	TGCCCTCGAGCCCACCAGGAACGAA
IL-6 R		CATAAGTTATGTGCCCAGTGGACAG
IL-10 F	659	ACATCAGGGGCTTGCTCTTGCTCGACC
IL-10 R		TGTCCCAGGGTCTAGTAGAGTCGCCA
IL-12p40 F	1118	GTTTCACACCCAGAAAACTGC
IL-12p40 R		ATATCTTTTCCGGGTCGATTAG

Table 3. GenBank Accession numbers used in the sequence comparison

Species	GenBank Accession Numbers					
	TNF-α	IL-2	IL-4	IL-6	IL-10	IL-12p40
Horse	NM_001081819	NM_001085433	NM_001082519	NM_001082496	NM_001082490	NM_001082516
Dog	EU_249361	AM_238655	AF_239917	NM_001003301	NM_001003077	NM_001003292
Cat	NM_001009835	NM_001043337	NM_001043339	NM_001009211	AF060520	NM_001077413
Cattle	EU_276079	NM_180997	NM_173921	NM_173923	NM_174088	NM_174356
Pig	NM_214022	NM_213861	NM_214123	NM_214399	NM_214041	NM_214013
Human	NM_000594	NM_000586	NM_172348	NM_000600	NM_000572	NM_002187

Table 4. Sequence identities between the horse, dog, cat, cattle, pig, and human cytokines

Cytokine	%Nucleotide(%Amino acid) identity					
	Horse	Dog	Cat	Cattle	Pig	Human
TNF-α	88.7(85.9)	88.1(88.8)	88.3(88.4)	83.2(78.1)	85.2(85.8)	88.6(86.7)
IL-2	79.3(65.8)	78.6(67.5)	82.1(71.2)	75.2(57.8)	80.9(68.0)	80.7(65.8)
IL-12p40	91.2(90.2)	89.4(87.2)	88.6(86.6)	89.1(88.1)	88.3(86.3)	89.1(86.9)
IL-4	76.0(60.6)	74.6(61.8)	76.0(63.9)	76.6(68.1)	80.2(67.7)	68.0(45.9)
IL-6	79.4(67.1)	77.1(62.6)	77.5(55.7)	73.7(55.5)	79.8(66.5)	76.2(60.8)
IL-10	92.1(89.3)	87.7(86.1)	88.6(84.1)	86.1(80.9)	84.1(79.2)	89.1(83.7)

REFERENCES

Calisher CH, Childs JE, Field HE, Holmes KV, Schountz T. 2006. Bats: important

    reservoir hosts of emerging viruses. Clin Microbiol Rev 19(3):531-545.

Chakraborty AK, Chakravarty AK. 1984. Antibody-mediated immune response in the

    bat, Pteropus giganteus. Dev Comp Immunol 8(2):415-423.

Chakravarty AK, Paul BN. 1987. Analysis of suppressor factor in delayed immune

    responses of a bat, Pteropus giganteus. Dev Comp Immunol 11(3):649-660.

Davis A, Bunning M, Gordy P, Panella N, Blitvich B, Bowen R. 2005. Experimental

    and natural infection of North American bats with West Nile virus. Am J Trop

    Med Hyg 73(2):467-469.

Hatten BA, Allen R, Sulkin SE. 1968. Immune response in chiroptera to bacteriophage

    phi-X174. J Immunol 101(1):141-150.

Hirano T, Yasukawa K, Harada H, Taga T, Watanabe Y, Matsuda T, Kashiwamura S,

    Nakajima K, Koyama K, Iwamatsu A. 1986. Complementary DNA for a novel

    human interleukin (BSF-2) that induces B lymphocytes to produce

    immunoglobulin. Nature 324(6092):73-76.

Hymowitz SG, O'Connell MP, Ultsch MH, Hurst A, Totpal K, Ashkenazi A, de Vos AM, Kelley RF. 2000. A unique zinc-binding site revealed by a high-resolution X-ray structure of homotrimeric Apo2L/TRAIL. Biochemistry 39(4):633-640.

Kidd P. 2003. Th1/Th2 balance: the hypothesis, its limitations, and implications for health and disease. Altern Med Rev 8(3):223-246.

Lam J, Nelson CA, Ross FP, Teitelbaum SL, Fremont DH. 2001. Crystal structure of the TRANCE/RANKL cytokine reveals determinants of receptor-ligand specificity. J Clin Invest 108(7):971-979.

Middleton DJ, Morrissy CJ, van der Heide BM, Russell GM, Braun MA, Westbury HA, Halpin K, Daniels PW. 2007. Experimental Nipah virus infection in pteropid bats (Pteropus poliocephalus). J Comp Pathol 136(4):266-272.

Nishihara H, Hasegawa M, Okada N. 2006. Pegasoferae, an unexpected mammalian clade revealed by tracking ancient retroposon insertions. Proc Natl Acad Sci U S A 103(26):9929-9934.

Odbileg R, Lee SI, Ohashi K, Onuma M. 2005. Cloning and sequence analysis of llama (lama glama) Th2 (IL-4, IL-10 and IL-13) cytokines. Vet Immunol Immunopathol 104(3-4):145-153.

Odbileg R, Lee SI, Yoshida R, Chang KS, Ohashi K, Sugimoto C, Onuma M. 2004. Cloning and sequence analysis of llama cytokines related to cell-mediated immunity. Vet Immunol Immunopathol 102(1-2):93-102.

Omatsu T, Watanabe S, Akashi H, Yoshikawa Y. 2007. Biological characters of bats in relation to natural reservoir of emerging viruses. Comp Immunol Microbiol Infect Dis 30(5-6):357-374.

Paul BN, Chakravarty AK. 1986. In vitro analysis of delayed immune response in a bat, Pteropus giganteus: process of con-A mediated activation. Dev Comp Immunol 10(1):55-67.

Swanepoel R, Leman PA, Burt FJ, Zachariades NA, Braack LE, Ksiazek TG, Rollin PE, Zaki SR, Peters CJ. 1996. Experimental inoculation of plants and animals with Ebola virus. Emerg Infect Dis 2(4):321-325.

Taniguchi T, Matsui H, Fujita T, Takaoka C, Kashima N, Yoshimoto R, Hamuro J.
1983. Structure and expression of a cloned cDNA for human interleukin-2.
Nature 302(5906):305-310.

Vieira P, de Waal-Malefyt R, Dang MN, Johnson KE, Kastelein R, Fiorentino DF,
deVries JE, Roncarolo MG, Mosmann TR, Moore KW. 1991. Isolation and
expression of human cytokine synthesis inhibitory factor cDNA clones:
homology to Epstein-Barr virus open reading frame BCRFI. Proc Natl Acad Sci
U S A 88(4):1172-1176.

Williamson MM, Hooper PT, Selleck PW, Westbury HA, Slocombe RF. 2000.
Experimental hendra virus infectionin pregnant guinea-pigs and fruit Bats
(Pteropus poliocephalus). J Comp Pathol 122(2-3):201-207.

Wolf SF, Temple PA, Kobayashi M, Young D, Dicig M, Lowe L, Dzialo R, Fitz L,
Ferenz C, Hewick RM. 1991. Cloning of cDNA for natural killer cell
stimulatory factor, a heterodimeric cytokine with multiple biologic effects on T
and natural killer cells. J Immunol 146(9):3074-3081.

Woolhouse ME, Gowtage-Sequeria S. 2005. Host range and emerging and reemerging
pathogens. Emerg Infect Dis 11(12):1842-1847.

Yokota T, Otsuka T, Mosmann T, Banchereau J, DeFrance T, Blanchard D, De Vries JE, Lee F, Arai K. 1986. Isolation and characterization of a human interleukin cDNA clone, homologous to mouse B-cell stimulatory factor 1, that expresses B-cell- and T-cell-stimulating activities. Proc Natl Acad Sci U S A 83(16):5894-5898.